Thesis, COLLÉGIALITÉ, FRANZEN Rachelle

Auteur : van Delft, Pauline
Promoteur(s) : Nguyen, Laurent; Javier Torrent, Míriam
Faculté : Faculté de Médecine
Diplôme : Master en sciences biomédicales, à finalité approfondie
Année académique : 2024-2025
URI/URL : http://hdl.handle.net/2268.2/23270

Master's thesis in Biomedical Sciences,
Multidisciplinary Research
2024 - 2025

LIÈGE université
Médecine

University of Liège, GIGA institute, Neuroscience

MECHANOTRANSDUCTION IN MIGRATING CORTICAL INTERNEURONS DURING NEUROGENESIS

Pauline van Delft

Supervised by Laurent Nguyen, promotor

and Míriam Javier-Torrent, co-promotor

Laboratory of Molecular Regulation of Neurogenesis

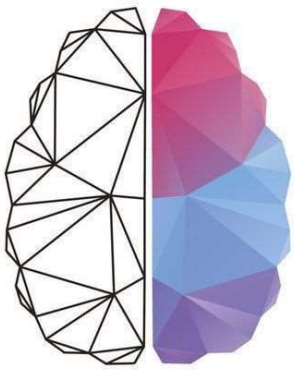

ACKNOWLEDGMENTS

First, I would like to sincerely thank Laurent Nguyen for welcoming me warmly into his laboratory. I am also deeply grateful to the truly amazing laboratory team, and I was very grateful to be part of it for a while.

Of course, I thank my family for their huge support throughout my studies, even if they still don't quite understand what I've been doing.
I also thank my friends for always standing by my side, and for their "constructive roasting" whenever I needed one. All these wonderful people I have met along this academic journey made these past years more meaningful and joyful.

Above all, I want to thank Míriam, who supported and guided me throughout this thesis. I am deeply grateful for her patience (especially with my tragic mental math skills), as well as for her constant enthusiasm. She has been the best supervisor I could hope for, and I am sincerely aware of how lucky I have been to work with her and to learn from her. I truly believe she is a remarkable researcher, the kind of researcher I aspire to become one day.

ABSTRACT (ENGLISH)

During brain development, migrating neuronal cells are subject to external forces coming from their surrounding microenvironment. These mechanical cues are transduced into intracellular biochemical processes (*i.e.* mechanotransduction), which regulate many cell responses, including migration behavior. However, interactions between cells and extracellular matrix (ECM) are not unidirectional, and neuronal cells migrating through the developing brain also display intrinsic mechanical forces on their substrate. In this master thesis, we investigate mechanotransduction regulation in cortical interneurons (cINs) migrating toward the neocortex. First, we demonstrate that inhibition of YAP/TAZ mechanosensors and transcriptional coactivators leads to migration defects in cINs. Secondly, we investigated the intrinsic mechanical forces exerted by cINs through Traction Force Microscopy (TFM), and highlighted intense traction forces around the axonal growth cone and soma. Eventually, we analyzed the brain ECM proteome from two neocortical zones where cINs migrate, the cortical plate (CP) and the subventricular/intermediate zone (SVZ/IZ), at two developmental stages (E13.5 and E16.5) through LC-MS/MS analyses. Our preliminary results highlight common proteins and differential expressions, including cell adhesion molecules and ECM proteoglycans, pointing toward new potential candidates for mechanotransduction regulation of cIN migration during neurogenesis.

RÉSUMÉ (FRENCH)

Au cours du développement cérébral, les cellules neuronales en migration sont soumises à des forces externes provenant de leur microenvironnement. Ces signaux mécaniques sont convertis en réponses biochimiques intracellulaires via la mécanotransduction, un processus qui régule de nombreuses fonctions cellulaires, dont le comportement migratoire. Toutefois, les interactions entre les cellules et la matrice extracellulaire (ECM) ne sont pas unidirectionnelles : les cellules neuronales exercent également des forces mécaniques intrinsèques sur leur substrat lorsqu'elles migrent à travers le cerveau en développement. Dans ce mémoire, nous étudions la régulation de la mécanotransduction au sein des interneurones corticaux (cINs) migrant vers le néocortex. Premièrement, nous démontrons que l'inhibition des mécanosenseurs YAP/TAZ, qui sont également des coactivateurs transcriptionnels, induit un défaut de migration chez les cINs. Deuxièmement, l'analyse des forces mécaniques intrinsèques exercées par les cINs par *Traction Force Microscopy* (TFM) a mis en évidence des forces de traction intenses au niveau du cône de croissance axonal et du soma. Enfin, nous avons analysé le protéome de l'ECM cérébrale dans deux zones néocorticales traversées par les cINs ; la plaque corticale (CP) et la zone subventriculaire/intermédiaire (SVZ/IZ), à deux stades embryonnaires (E13.5 et E16.5) par analyses LC-MS/MS. Nos résultats préliminaires mettent en évidence des protéines communes et des expressions différentielles, incluant des molécules d'adhésion cellulaire et des protéoglycanes de l'ECM, et suggérant ainsi de nouveaux candidats potentiels dans la régulation mécanotransductionnelle de la migration des cINs au cours de la neurogenèse.

ABBREVIATIONS

CGE	Caudal Ganglionic Eminence
CNS	Central Nervous System
cIN	Cortical Interneuron
CP	Cortical Plate
E	Embryonic day
ECM	Extracellular matrix
FAs	Focal Adhesion's
GE	Ganglionic Eminences
GFP	Green-Fluorescent Protein
IN	Interneuron
IZ	Intermediate Zone
LGE	Lateral Ganglionic Eminence
MGE	Medial Ganglionic Eminence
MZ	Marginal Zone
PN	Projection Neurons
SVZ	Subventricular Zone
TAZ	Transcriptional co-Activator with PDZ-binding motif
TFM	Traction Force Microscopy
VZ	Ventricular Zone
YAP	Yes-Associated Protein

INDEX

INTRODUCTION

1. INTRODUCTION

1.1. Introduction to mouse embryonic brain

In mice, gestation period extends over approximately 18.5 embryonic days (E). The development of central nervous system (CNS) begins from E8.5 with the formation of the neural tube, originating from the neuroectoderm.[1,2] This primary structure will develop into transient anatomic regions: the prosencephalon (that will give rise to the telencephalon and diencephalon), the mesencephalon, and the rhombencephalon.[1,3]

The telencephalon is subdivided into two main areas: the pallium (or dorsal telencephalon) and the subpallium (or ventral telencephalon), in which this master thesis is focused. The pallium includes the hippocampus, the olfactory system, and the 6-layered neocortex.[1,3]

1.1.1. Corticogenesis

The mouse cerebral cortex is a remarkably complex structure in terms of its function, composition, and development. In mammals, the cortex is the seat of higher cognitive functions, including the integration of sensory and motor information, memory, and emotional processing.[4,5]

During development, the neocortex is organized into several germinative and transitory zones: the ventricular zone (VZ), subventricular zone (SVZ), intermediate zone (IZ), cortical plate (CP), and marginal zone (MZ), from deep to superficial, respectively. The VZ contains the principal pool of neural stem cells – initially neuroepithelial cells, and later radial glial cells – which serve as the main source of locally generated neurons within the cortex. The SVZ is a proliferative zone rich in intermediate progenitors derived from RGCs. The IZ constitutes a transitional zone traversed by growing axonal fibers and serves as a migratory route for neurons originating from distant regions, such as the ventral telencephalon.[3,6] The CP represents the final destination of migrating postmitotic neurons, and will develop in an inside-out fashion into cortical layers II to VI.[5-7] Finally, the MZ plays a crucial role by secreting molecular cues essential for cortical development, and is the primordium of layer I.[1,8]

These transient embryonic zones guide the proliferation, migration and positioning of neural cells travelling to their final cortical layer. Neurons populating the cerebral cortex notably include projection neurons (PNs), born locally in the VZ and SVZ, and interneurons (INs), originating from the subpallium.[4]

Basal to the pallium, the subpallium includes the ganglionic eminences (GEs). These transitory embryonic structures can be subdivided into lateral (LGE), medial (MGE), and caudal (CGE) parts. While the CGE is located in the caudal part of the developing brain, the LGE and MGE form distinct bulges in a more rostral region (**Fig. 1**).[1-4] During neurogenesis, LGE produces PNs that will migrate to the striatum and the olfactory bulbs, while the MGE and CGE contribute actively to the development of the brain, and more particularly to the neocortex.[1,9] Indeed, these two regions contain progenitors of GABAergic interneurons and oligodendrocytes that will progressively populate the cerebral cortex.[9] Particularly, cortical interneurons (cINs) arise from the MGE – and to a lesser extent, from the CGE – and migrate towards the CP. Early-born INs settle in the deepest layers (VI, V, IV), while late-born cINs migrate past them to populate progressively more superficial layers (I, II, III), resulting in the cortical stratification.[6-8,10]
Later during development, the MGE and CGE continue their growth and give rise to the globus pallidus and the amygdala body, respectively.[1,4] The rodent cortex continues to mature during several postnatal days through coordinated cellular and molecular processes, including neuronal migration, differentiation, and programmed cell death, which together contribute to the proper establishment of neocortical architecture.[2,11]

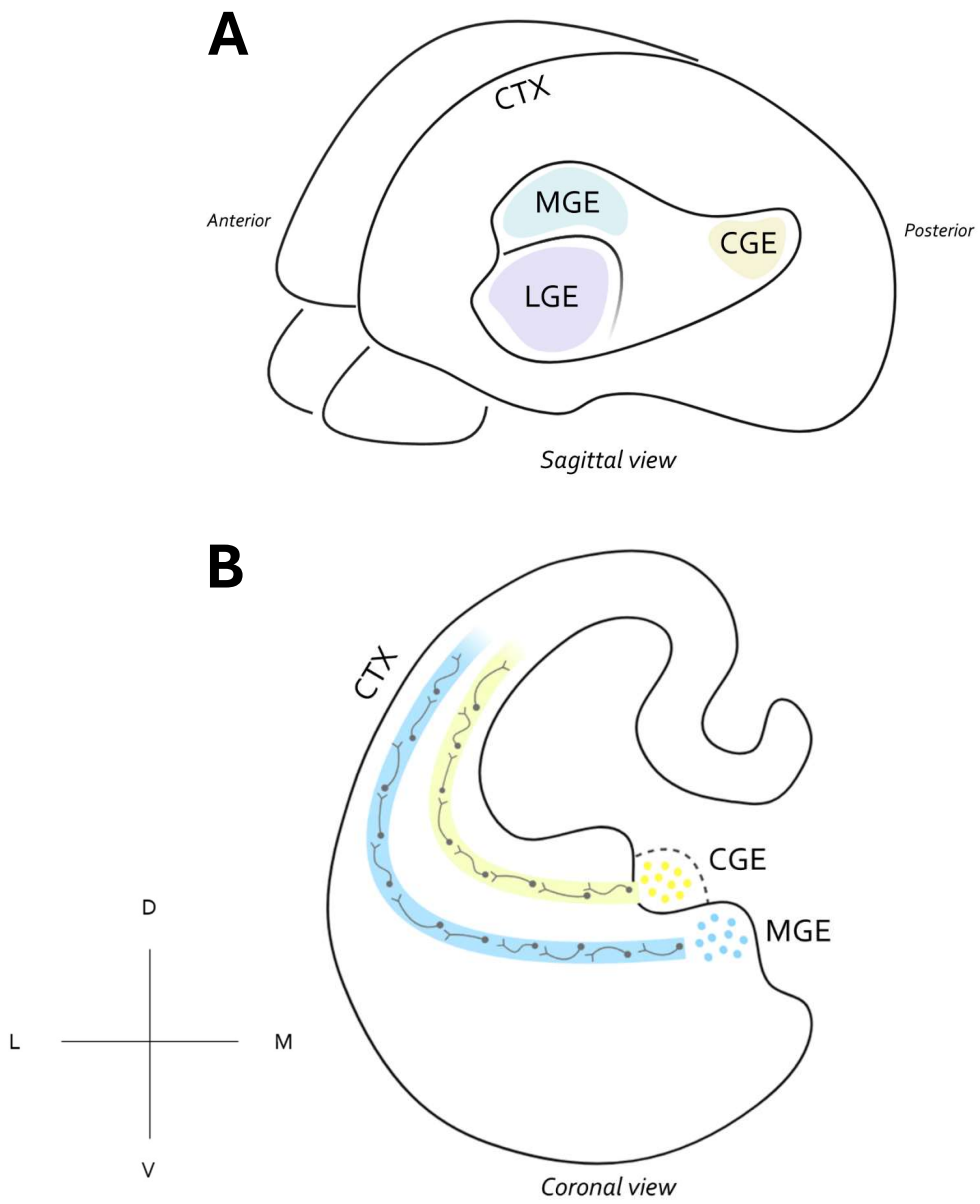

Figure 1: ***Schematic representation of embryonic mouse telencephalon***. ***A)*** *Sagittal view of mouse telencephalon.*[4] ***B)*** *Coronal view of mouse telencephalon . Neurons are migrating from CGE and MGE towards the cortex. CTX = cortex, CGE = caudal ganglionic eminence, LGE = lateral ganglionic eminence, MGE = medial ganglionic eminence, D = dorsal, L = lateral, M = medial, V = ventral.*

1.1.2. Neural cells

The cerebral cortex is ultimately composed of a diverse array of neurons – hundreds of subtypes – that have migrated across the transient embryonic zones to reach their appropriate cortical layer and establish functional cortical circuits.[4]

Within this heterogeneous population of cortical neurons, PNs and INs play a central role in maintaining the balance between excitation and inhibition, which is essential for the proper cortical activity.[12] These two major categories of neurons differ in several fundamental aspects, including their developmental origin (as previously discussed), mode of migration, differentiation pathways, morphology, connectivity, electrophysiological properties, and the neurotransmitters they release.[13]

1.1.2.1. *Cortical projection neurons*

PNs are excitatory cells that release glutamate, the main excitatory neurotransmitter in the CNS. They constitute approximately 80% of total cortical neurons in rodents.
Morphologically, PNs display a pyramidal shape and long myelinated axons that project over long distances. This morphology enables them to connect several brain regions or structures, allowing the transmission of excitatory signals to distant targets.[14]
During neurogenesis, PNs are generated locally within the pallium and migrate over short distances via radial migration, using radial glial fibers as a scaffold to reach the cortical plate.[4,9,13]

1.1.2.2. *Cortical interneurons*

cINs, in contrast, are inhibitory neurons that synthesize gamma-aminobutyric acid (GABA). The main role of cINs is to modulate the local activity of cortical circuits and to prevent excessive excitatory activity.[13,15,16]

Immature cINs present a highly dynamic bipolar morphology, characterized by a long leading process that extends from the apical side of the soma.[17] When INs settle in the CP, they progressively acquire their mature configuration, which depends on their specific subtype and

function. cINs stereotypically exhibit short, unmyelinated short axons, and an elaborated axonal and dendritic arborization.[15] The rich arborization of cINs enable them to target nearby PNs – and other INs – within the neocortex.[18,19] Synaptic connections can be established on different subcellular compartments of the postsynaptic neuron, including axonal and initial segments, soma, or dendrites, resulting in distinct effects.[12,19] In the synaptic cleft, GABA neurotransmitter is released by the presynaptic IN and binds to $GABA_A$ receptors. This causes membrane hyperpolarization in the postsynaptic cell, and consequently to the inhibition of action potential firing.[15,16] During neonatal development, however, it is worth noting that GABA presents excitatory effects, promoting calcium signaling and playing critical roles in guidance and migration of immature neurons.[12] In addition to the establishment of inhibitory connections, cINs are key regulators of electrical activity across neural circuits, and are responsible for the synchronization of neuronal circuits, which is essential for higher-order cortical functions.[18]

Although they represent only 20% of the total cortical neuron population, INs display remarkable diversity, with more than 50 distinct subtypes that can be identified based on morphology, electrophysiology, and transcriptomic.[12,18,19] Commonly, three main cardinal categories are used to classify cINs: parvalbumin (PV), somatostatin (SST), and serotonin-receptor 5HT3a (5HT3aR), which can be further divided into distinct subtypes.[12,18]

Given their complex but crucial roles, cINs are implicated in a wide range of neurodevelopmental disorders. For instance, mutations affecting genes involved in development, differentiation, or function of cINs contributes to imbalances in excitatory and inhibitory signaling. Among the key steps in cIN development, proper migration from the MGE/CGE to the cortex is essential, and defects in migration have been associated with disorders such as epilepsy, autism spectrum disorders (ASD), schizophrenia, and severe neurodevelopmental phenotypes.[12,15,18] Therefore, investigations on mechanical cues underlying cIN migration could lead to relevant insights into the etiology of these disorders.

1.1.2.3. *Glial cells*

Neurons are not the only cell type populating the brain. Neuroglia represent approximately half of all cells in the rodent CNS and play essential roles in its development and function. Glia are categorized into three main types: astrocytes, oligodendrocytes, and microglia.

Oligodendrocytes are responsible for the myelination of long axons, particularly those of PNs. Microglia are the resident immune cells of the CNS, and are involved in immune surveillance, phagocytosis of cellular debris, and modulation of inflammatory reactions under pathological conditions. Astrocytes provide both metabolic and structural support to neurons, and modulate synaptic activity by recycling neurotransmitters such as glutamate and GABA.

Together, glial cells influence neuronal birth, migration, and axonal growth during neurogenesis, as well as synaptic communication, plasticity, and homeostasis in the mature CNS.[20,21]

1.2. Cortical GABAergic interneurons

cINs originate mainly from the MGE, although the CGE contributes to approximately 30% of the population. The place and time of birth of cINs depend on their subtype identity. SST^+ and PV^+ interneurons are generated early, around E11, and derive primarily from the MGE.[12] The production of SST^+ interneurons declines rapidly and ceases around E14, whereas PV^+ interneurons are generated over a more extended period, approximately until E18. $5HT3aR^+$ neurons, however, arise later during development (around E13) from the CGE. It is worth noting that a small amount of cIN subpopulations originate from the preoptic area (POA), mostly PV^+ and SST^+ cells.[15] In this master thesis, we focus on the MGE structure, which gives rise to SST+ and PV+ cINs.

From the subpallium GEs, cINs undergo long-distance tangential migration to reach the neocortex, mainly following two distinct streams within the pallium; one in the SVZ/IZ, and one in the CP.[7,10,19,22]

It has been demonstrated that the migratory route used by cIN depends notably on their subtype. While the vast majority (~70%) migrate through the SVZ/IZ, some subpopulations

show a preference for alternative pathways. Notably, a subset of SST^+ INs migrate through the CP. This choice of migratory stream appears to be subtype-specific and may influence their subsequent maturation.[10] Therefore, it has been suggested that the microenvironment encountered along each route contributes to subtype differentiation. Interestingly, transcriptomic analyses have demonstrated that cINs migrating through the CP exhibit a distinct molecular profile to those transiting in the SVZ/IZ.[23]

After cINs have reached their proper cortical region by tangential migration, they start migrating radially to reach their final laminar position within the CP.[4,18,19]

1.2.1. Migratory behavior of cortical interneurons

From a cellular point of view, tangentially migrating cINs undergo saltatory nuclear movements. This saltatory progression is defined as nucleokinesis and comprises three major steps; elongation of the leading process, followed by nucleus migration into this newly formed structure, and finally retraction of the trailing process (***Fig. 2***). This three-steps cyclic process can be subdivided into two phases; resting phase, when cytoplasmic organelles are migrating into the leading neurite, and the dynamic phase, when the nucleus translocate towards the dislocated organelles. Each step is controlled by the cytoskeleton – more particularly by actin filaments and microtubules – which allows the synchronization of both phases and the correlation between neuritic elongation and nuclear migration.[7,17]

During the first step of nucleokinesis, cINs elongate their leading process and extend branching to sense the environment. Once the leading neurite has stabilized in a specific direction according to the extracellular signals, the resting phase begins with the segregation of centrosome and Golgi apparatus from the perinuclear compartment. The dissociated organelles migrate at a large distance from the nucleus and reassociate in the leading neurite, forming a swelling at the front to the nucleus. Microtubules play a crucial role in this first phase by creating pulling forces at the leading edge of the migrating cell, supporting the extension of the leading process. In addition, microtubule cytoskeleton supports the initiation of the second phase by coupling the centrosome to the nucleus, facilitating nuclear translocation.[17]

The dynamic phase of nucleokinesis in migrating MGE cells is associated with an accumulation of myosin-II behind the nucleus, forming a trailing process. The contraction of myosin allows the nucleus to jump towards the dislocated organelles, into the swelling. Therefore, the second phase rests on actomyosin-dependent pushing forces at the rear of the cell, additionally to the anterograde attraction from microtubule network. [17]

This two-phase cyclic behavior generates the saltatory progression of the tangentially migrating cIN. Nucleokinesis in cINs generally lasts between 3 and 9 minutes. The nucleus typically leaps on a distance of 5-25 µm, with a mean speed of 35 µm/h. Studies have demonstrated that these properties of migrating MGE cells are conserved *in vitro*.[17]

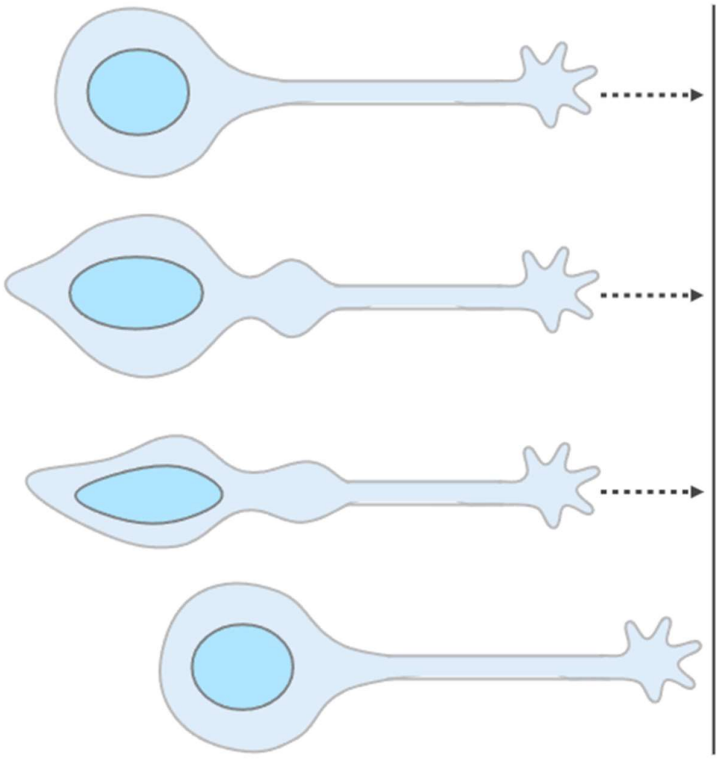

***Figure 2**: **Schematic representation of cIN nucleokinesis**. During tangential migration of cortical interneurons, the centrosome moves forward, pulled by microtubule motors. The nucleus follows through actomyosin forces at the rear of the cell.*

1.2.2. Molecular mechanisms regulating cortical interneurons migration

The migration of cINs into the developing cortex is tightly regulated by a combination of molecular mechanisms, both intrinsic and extrinsic. Extrinsic signals include notably chemotactic gradients and mechanical cues from the surrounding environment, while intrinsic mechanisms particularly involve the regulation of cytoskeletal dynamics and genetic programs within the cell. Together, these signals ensure proper directionality, motility, and integration of interneurons into the cortical networks.[24]

1.2.2.1. *Genetic programs*

Tangential migration of cINs is orchestrated by specific genetic programs that underlie intrinsic mechanisms, such as cytoskeletal remodeling and nucleokinesis.

The *Distal-less* (DLX) family of homeodomain transcription factors includes six members (*Dlx1* to *Dlx6*) that play central roles in regulating the fate and migration of cINs.[9,12,19] These transcription factors are sequentially and spatially expressed throughout development. At early embryonic stages, *Dlx1* and *Dlx2* are strongly expressed in the MGE and CGE, where they are required for the initiation of cIN migration. Later, they activate *Dlx5* and *Dlx6*, which promote cIN motility, notably by regulation actin cytoskeleton remodeling. These later-expressed transcription factors are reliable markers commonly used to identify cINs originating from MGE and CGE.[9,15,19]

DLX transcription factors induce the expression of downstream transcriptional regulators, such as *Lhx6* and *Arx*, which also play central roles in cIN migration and are enriched in specific regions of the developing neocortex.[19]

Disruption of *Dlx* genes results in profound migratory defects. More particularly, *Dlx1/2* knockout mice exhibit accumulation of cINs in the subpallial zones, due to failed initiation of tangential migration. *Dlx5/6* mutants show impaired migration and a reduced number of cINs in the cortex, highlighting the indispensable role of these transcription factors in guiding INs to their final destinations.[4,9,12]

1.2.2.2. *Chemical regulation*

Chemicals cues are continuously secreted by brain cells in the microenvironment and affect interneuron development in many ways. Particularly, tangentially migrating cINs respond to gradients of attractive and repulsive chemicals (also called morphogens) that are essential to maintain proper migratory routes and ensure accurate spatial and temporal positioning of cINs within the developing cortex.[24]

Repulsive chemical cues play a crucial role in preventing cINs from entering inappropriate regions during their migration, and in promoting their exit from proliferative regions. These signaling molecules typically act through interaction with membrane receptors expressed by cINs and trigger intracellular cascade, resulting in a tight regulation of migration key mechanisms.[4]

For instance, Sema3A/3F are expressed in the striatum, and Npn-1/2 are expressed by cINs; this signaling mechanism avoid cINs to migrate towards the striatum.[12,19,24-26] Similarly, Slit1/2 and EphrinA5 proteins are expressed in the VZ and interact with Robo and EphA4 receptors, respectively, on migrating cINs.[27] There, they exclude cINs from proliferative zones, indirectly directing them towards permissive zones for migration, such as SVZ/IZ. In addition, Cajal-Retzius cells located in the MZ secrete Reelin. This glycoprotein acts as a "stop" signal for migrating neurons as they approach the CP, preventing their premature integration. Moreover, Reelin promotes cell-matrix adhesion, which is critical for tangential migration.[12,28,29]
In addition to repulsive cues, gradients of attractive morphogens also play a central role in directing cINs from subpallial regions towards their proper destinations in the developing pallium. Among these attractive cues, Neuregulin 1 (Nrg1), secreted by pallial cells, act as strong attractant by binding to ErbB4 receptors, which are expressed by the majority of cINs at perinatal stages.[12,19,29,30] Plus, gradients of chemokines, such as Cxcl12, are secreted by intermediate progenitors and by the meninges, and help to locally retain cINs within these permissive migratory pathways. [29-33]

Molecules typically involved in neurotransmission in adult mammalian brain, such as GABA (among others), can act as morphogens during embryonic development.[2,19,34] By binding to $GABA_A$ receptors expressed on cINs originated from the MGE, GABA exerts a tonic influence along their migratory path. This signaling increases both cell motility and the frequency of nucleokinesis events. These effects are attributed to GABA's transient excitatory action during embryogenesis stages.[12,34]

The effects of morphogens on cINs migration are tightly regulated by the temporal expression of their corresponding receptors, which vary across development stages. This dynamic expression ensures that INs respond appropriately to guidance cues, which are crucial for proper neuronal migration. Disruption of these signaling pathways, such as through mutation in guidance receptors, leads to severe migratory defects, highlighting the essential role of morphogen gradients in regulating the precise spatiotemporal migration of cINs.[19,35]

1.2.2.3. *Mechanical signals*

During embryogenesis, a period characterized by intense tissue remodeling and growth, neurons encounter numerous mechanical stimuli coming from their surrounding environment. External mechanical cues refer to passive mechanical properties of the environment, as well as active external forces exerted by neighboring cells.[36,37]

Recent studies by *Leclech et al*. demonstrated that migrating cINs responds dynamically to topographical cues in their environment. Using substrates with defined geometrics, such as micropillars, round, or squares spaces, the authors showed that physical constraints can influence the morphology and migration of cINs. Their findings support that natural tissue topography, including the organization of blood vessels, axons, and other anatomical structures, can orient or constrain the directionality of migrating cells.[38]

In addition to topography, spatial confinement, due to cellular or local cell density or ECM composition, also modulates migration dynamics; low-connected or low-density tissue allows easier movement, while dense tissue limits cell motility.[36,37,39,40]

Moreover, the ECM architecture – filament and fibrillar organization – serve as a physical scaffold guiding cell migration.[36,37]

On the other hand, active mechanical forces arise from interactions with neighboring cells. For instance, local glial cells, axons, or other migrating neurons can exert compression, tension, or shear forces on cINs. Furthermore, communication of cINs with other cells, such as PNs and microglia, influences their migration, principally via the establishment of physical contacts.[40]

These external mechanical signals are transmitted to cINs mainly through adhesion complexes, such as cell-cell junctions, and cell-matrix interactions. These structures do not only act as mechanosensors that relay external forces inward; they also serve as mechanical anchors through which cINs exert intrinsic forces on their environment. Indeed, communication through adhesions is bidirectional, allowing migrating INs to perceive but also to actively respond to mechanical stimuli.[36,40] The generation of intrinsic forces by cINs and their influences on migration will be explored in later sections.

1.3. MECHANOBIOLOGY

Mechanobiology is at the core of this master's thesis, which investigates the mechanical interactions between migrating cINs and the embryonic brain environment. In this section, we describe the mechanical properties of both the ECM and migrating cINs, and discuss the mechanotransduction mechanisms that mediate their interactions.

1.3.1. Mechanobiology of mouse embryonic brain

Brain tissue is typically softer than other tissues, and stiffness varies within cortical regions and across developmental stages.[36,40] Particularly, SVZ/IZ is generally softer at early stages, but stiffness increases through development. Similarly, the tissue stiffness of the CP also increases, but become softer at later stages.[41,42] ECM stiffness is an essential property for cell differentiation, migration, and mechanotransduction. This is determined by structural organization, cell density, as well as molecular composition.[36,40]

Specific brain ECM components include hyaluronic acid, elastin, and numerous proteoglycans, which provide structural support and define basement membranes within the tissue. For

instance, chondroitin sulfate proteoglycans (CSPGs) are particularly enriched in the VZ, where they influence neuronal migration by acting as binding sites for various guidance molecules. CSPGs interact with Semaphorin 3A, influencing the migratory path of cINs.[37,43]

Laminins are additional major ECM components, forming the basal lamina around the brain and cerebral blood vessels, and contributing to the structural integrity of the blood-brain barrier. Specifically, laminin-γ1 is expressed in cINs and helps directing their migration towards the MZ. Laminins interact intensively with integrin receptors, mediating essential cell-ECM signaling that underlies numerous neuronal processes. [37,44]

Other important ECM components include fibronectin, which facilitates cell adhesion, and collagen, which facilitates directional migration. While fibronectin is present from early stages, collagen accumulates later during development and contributes to increased tissue stiffness, density and structural organization, thereby progressively limiting cell motility as it accumulates in the ECM.[37]

The composition of ECM is highly dynamic and undergoes constant remodelling to meet the needs of neural cells. In early stages of brain development, the ECM is typically sparse in fibers, creating a permissive environment that facilitates rapid cell migration. Later, as development progresses, the ECM becomes increasingly enriched in structural proteins, such as laminins and collagens. This maturation is also accompanied by more complex tissue organization and the accumulation of ECM proteins secreted by surrounding cells, such as Reelin and myelin-associated components arising from axonal myelination at later stages. ECM remodelling implies multiple mechanisms.[36,37,40,45]

First, the secretion of new ECM components by surrounding cells – migrating neurons, glial cells, and endothelial cells – often through exocytosis of extracellular vesicles (*i.e.* exosomes) contribute to the remodelling of ECM. Additionally, local ECM degradation is mediated by matrix metalloproteinases (MMPs), which are able to cleave ECM components. These enzymes are also secreted by cells, in order to facilitate their way through the environment while migrating.

Plus, post-translational modifications of ECM molecules, such as the sulfation or desulfation of CSPGs, modulate their affinity and interactions with guidance molecules, regulating ECM properties. Finally, interactions with cell surface receptors, notably integrins, can also mediate adhesion and lead to modulation of local ECM composition. [37]

Importantly, abnormal changes in expression of ECM components can interfere with proper brain development.[36] Mutations in genes encoding ECM components are associated with neurodevelopmental disorders and cortical malformations, emphasizing the critical role of ECM in brain development. Particularly, loss of function mutations of laminins – or their receptors – can be involved in lissencephaly.[36,44,46]

1.3.2. Mechanobiology of neural cells

Rather than being passive responders to environmental cues, neurons actively generate mechanical forces that influence their migration and interaction with the ECM. Indeed, neuronal migration is regulated by intrinsic mechanical mechanisms that are essential to both nucleokinesis and exploratory behavior of migrating neurons.[36,47,48]

For instance, at the leading edge, cINs extend dynamic extensions driven by actin polymerization, generating protrusive forces that facilitate microenvironmental sensing. Microtubule polymerization also enables the extension of exploratory branches that dynamically project and retract, contributing to active exploration.[36,48,49,50] Nucleokinesis can be described as a balance of internal pushing and pulling forces. At the front of the cell, the leading neurite – and particularly the growth cone – generates pulling forces to translocate the nucleus forward.[17,36,48,49] This is accompanied by traction forces, that are transmitted to the substrate through clutches – such as shootin1b, in olfactory INs – that link the cytoskeleton to the ECM (**Fig. 3**).[51]

Altogether, intrinsic forces generated by cINs are tightly coordinated and dynamically regulated, forming a bidirectional mechanical dialogue with the ECM and the neighboring cells, which is essential for effective migration.[36,37]

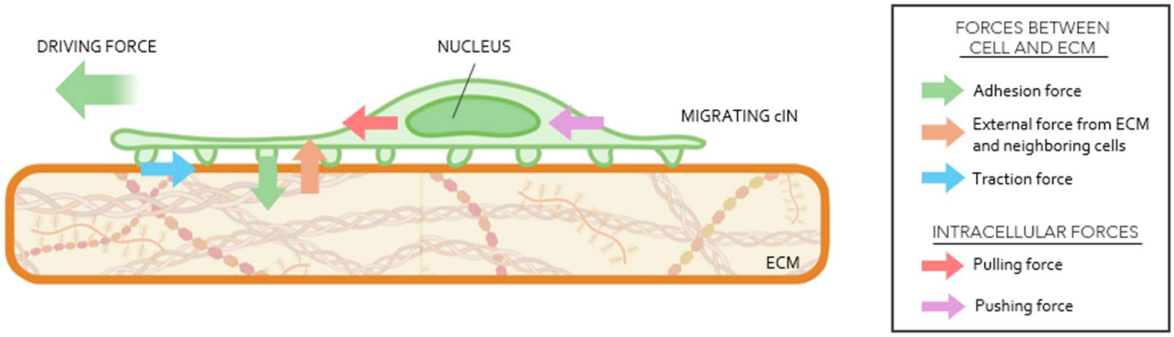

***Figure 3*: Schematic representation of traction forces between migrating cIN and ECM.** Intracellular forces are displayed by the migrating cIN and are mediated by cytoskeleton remodelling. Intrinsic forces are transmitted to the ECM, which also exerts dynamic forces on the cIN.

1.3.3. Cellular mechanotransduction

Mechanotransduction refers to the process by which cells convert external mechanical stimuli into intracellular biochemical signals, enabling them to adapt their behavior to the mechanical properties of their environment. According to the mechanical clutch model, cells first sense the mechanical cues and respond to them via dynamic connections with the cytoskeleton. Mechanosensors include a wide range of proteins, such as adhesion molecules, cell-cell junctions, stretched activated ion channels, and some tyrosine-kinase receptors.[47,52,53]

The transmission of tension across membrane often triggers the recruitment and activation of intracellular signaling molecules, such as focal adhesion kinase and Src-family kinases. Often, these molecular signals within the cytoplasm are transmitted to the nucleus to regulate the expression of genes.[47,54]

Particularly, focal adhesions (FAs) play a pivotal role in mechanotransduction. These are multiprotein complexes present at the cell-ECM interface, connecting ECM components to the actin cytoskeleton principally through integrins. These heterodimeric receptors bind specifically to ECM components such as fibronectin, collagen, or laminin and allow the transduction of mechanical cues into biochemical signals through outside-in and inside-out signaling. Upon ligand binding, integrins undergo conformation changes, promoting recruitment of adaptor proteins like talin, vinculin, or paxillin, which are coupled with actin filaments. These macrocomplexes act as mechanosensors and provide a link between the cytoskeleton and the ECM.[47,54,55,56]

Moreover, mechanical signals can be transmitted to the nucleus via the Linker of Nucleoskeleton and Cytoskeleton (LINC) complex [44,57]. Eventually, transmission of forces to the nucleus can influence chromatin organization and gene expression. Therefore, the nucleus of migrating cells is subjected to significant external and internal mechanical stress, and the nuclear envelope acts as a mechanosensitive surface through the LINC complex, the actin filaments, intermediate filaments and microtubules, connecting the nuclear envelope to the cytoskeleton [54,57,58].

1.3.4. Mechanosensors: YAP/TAZ

Yes-associated protein (YAP) and its transcriptional co-activator with PDZ-binding motif (TAZ) are key transcriptional coactivators of the Hippo pathway, and are involved in controlling cell proliferation, differentiation, survival, and migration. In the nucleus, they interact with TEA domain transcription factors (TEADs) to drive the expression of targeted genes (**Fig. 4**). Activation of Hippo pathway leads to the sequential phosphorylation of upstream kinase, eventually leading to phosphorylation of YAP/TAZ by LATS1/2 kinases. This leads to YAP/TAZ cytoplasmic sequestration by protein complexes, before being ultimately degraded by the proteasome. [47,59,60,61]

Yap1 activity is also regulated by mechanical cues. Upon force application – such as ECM rigidity, shear stress, or increased adhesion – mechanical deformation of nuclear pores facilitates Yap1 nuclear translocation.[62] This mechanical regulation depends tightly on cytoskeletal components within the cell, and cell-ECM adhesion complexes. While several studies highlight Yap1 sensitivity to substrate stiffness,[60,63,64] others suggest that cell density also modulates its localization and activity.[65] Moreover, it has been demonstrated that calcium-dependent pathways, including those triggered by activation of mechanosensitive Piezo channels, promote Yap/Taz activation as a downstream effector.[66]
Importantly, Yap1 acts as both a mechanosensor – responding to extracellular mechanical cues through nucleus translocation – and a mechanotransducer, as it subsequently modulates gene expression to modulate cell behavior in response to the mechanical stimuli.[64]

Recent works indicate that Yap1 promotes neuronal specification versus glial fate in response to substrate stiffness in human stem cells.[67] Of interest, the potential of YAP/TAZ as a key mechanosensor in migrating neurons have been proposed. Indeed, interesting work from our laboratory has shown that *Yap1* is differentially expressed in migrating cINs at different embryonic stages (data not shown). Yet, little is known about their precise function in the context of cIN migration during embryonic development. A better understanding of how YAP/TAZ respond to the mechanical properties of the brain and mediate intrinsic mechanisms

of regulation could shed light on the fundamental principles governing cIN migration during embryogenesis.

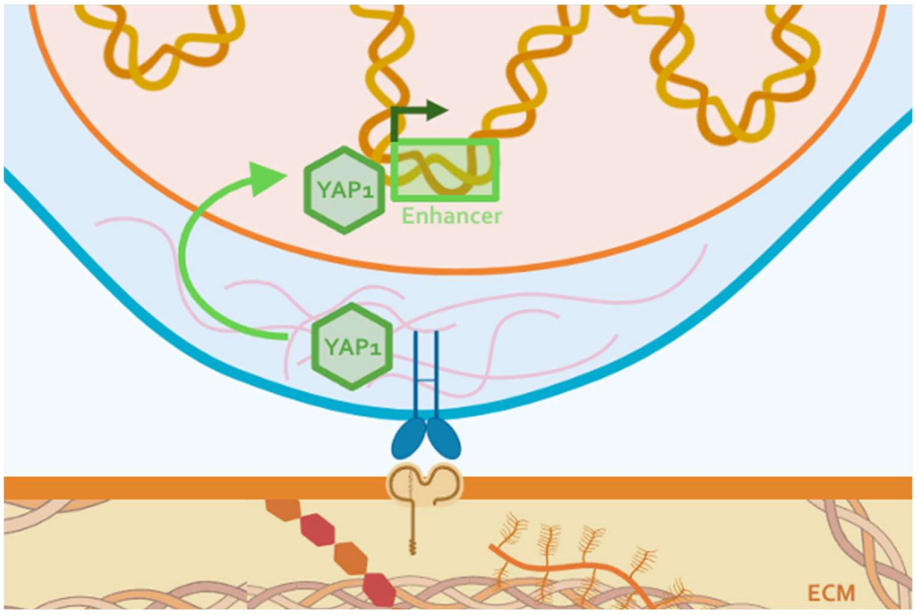

***Figure 4*: Schematic representation of YAP/TAZ signaling in response to mechanical cues from the ECM**. *Mechanical cues from the ECM are sensed by cIN through mechanosensors. These mechanical stimuli leads to translocation of Yap1 to the nucleus, where it binds to transcriptional activators to regulate the expression of genes.*

OBJECTIVES AND EXPERIMENTAL STRATEGY

2. OBJECTIVES AND EXPERIMENTAL STRATEGY

The main objective of this thesis is to study the mechanotransduction regulation of cortical GABAergic interneuron migration through cortical development.

Objective 1: To study the contribution of YAP/TAZ to the migration of cINs.

YAP1 is a transcription coregulator known to exhibit mechanosensing and mechanotransducing properties. Preliminary data indicates that *Yap1* is downregulated in cINs through development (data not shown). Thus, we want to investigate if this mechanotransduction candidate might modulate the IN migratory behavior. In order to study its role in cINs, we inhibited Yap1 in cultured E13.5 MGE explants and performed time-lapse imaging of migrating neurons.

Objective 2: To investigate the intrinsic mechanical forces generated by the cINs during their migration.

Migration of cINs involves exploration behavior through the actin cytoskeleton within the leading neurite [ref]. Here, we want to characterize the mechanics behind the extension of the leading process and to investigate the traction forces generated by cINs on their substrate. MGE explants from E13.5 and Dlx5,6-Cre:GFP-positive mouse embryos were cultured on a polyacrylamide hydrogel containing fluorescent microbeads, allowing the measurement of the forces using traction force microscopy (TFM).

Objective 3: To identify the ECM content of the migratory streams of cINs during development.

Emerging evidence indicate that migrating neurons during neurogenesis are sensitive to changes in the environment. To better understand the impact of the extracellular environment on the way cINs are migrating, we aim to investigate the ECM composition in the two migration pathways, namely the CP and the SVZ/IZ. This will allow us to highlight potential differences of protein content in both zones and during distinct stages of the development. In order to identify the proteins in the ECM, we performed mass spectrometry on laser microdissected tissue within the two cortical regions, at E13.5 and E16.5.

MATERIALS AND METHODS

3. MATERIALS AND METHODS

3.1. MOUSE MODELS

To obtain Dlx5,6-Cre:GFP-positive embryos, wild-type *Swiss* females were crossed with Dlx5,6-Cre:GFP-positive *Swiss* males. Pregnant females were sacrificed by cervical dislocation at embryonic day (E) 13.5 or 16.5 in order to collect Dlx5,6-Cre:GFP-positive embryos, following the guidelines from the *Ethical Committee* of the *University of Liège* (protocol 20-2231).

3.2. CELL CULTURE

3.2.1. ECM coating

3.2.1.1. *Poly-L-ornithine and laminin*

4-compartment dishes were coated with 0.1 mg/mL poly-L-ornithine (#P4638 *Sigma-Aldrich*, diluted in water) for 45 minutes at 37°C. This was followed by a treatment with 20 µg/mL laminin (#L2020 *Sigma-Aldrich*, diluted in DPBS) for 2 hours at 37°C.

3.2.1.2. *N-cadherin / Fibronectin*

The coating was performed by the application of poly-L-ornithine (#P0899-100mg, *Sigma-Aldrich*) at 1 µg/µL in PBS, incubated in 4-compartments dishes for 2 hours at 37°C. The compartments were then washed three times in DPBS (*Dulbecco's Phosphate Buffered Saline*, #L0615, *Biowest*) before undergoing an overnight treatment at 37°C with 4 µg/100 µL anti-FC (goat anti-mouse IgG Fc specific, #M4280-1ML, *Sigma-Aldrich*) in 0.1 M Borate Buffer (pH 8.5). The following day, the compartments were washed three times with Borate Buffer.

Afterwards, the coating was completed with 10 µg/mL of N-cadherin-FC chimera protein (recombinant mouse, #6626-NC-050, *R&D Systems*) and 10 µg/mL of Fibronectin (#F-4759, *Sigma-Aldrich*), incubated in Borate Buffer for 2-3 hours at 37°C. The compartments were then washed thrice in DPBS before incubation at 37°C.

3.2.2. Cortical feeder

In order to obtain the best substrate for interneurons migration, a homochronic layer of cortical cells (*i.e.*, cortical feeder) was prepared from E13.5 embryos. All dishes were previously coated

with poly-L-ornithine and laminin as described before. For every 4-compartment dish, 1.5 embryos were dissected.

Brain cortices were isolated and placed in 600 µL of Neurobasal (NB) medium (#21103-049, *ThermoFisher*) supplemented with 1% Penicillin-Streptomycin (#11548876, *Gibco*), 1% B27 (#17504044, *Gibco*), 0.5% N2 (#17502048, *Gibco*), and 0.5% *GlutaMAX* (#35050-038, *Gibco)*. Mechanical dissociation was performed by gently pipetting up and down and the resulting solution was then filtered with 40 µm filters to remove meninges and no dissociated tissue. Cortical cells were then maintained at 37°C, 5% CO_2 for 24 hours before deposition of the MGE explants.

3.2.3. MGE explants

The MGEs from E13.5 embryos were isolated and dissected into small explants in HBSS (*Hanks' Balanced Salts Solution* #L0612-500, *Biowest*). MGE explants were seeded in 4-compartments dishes containing a cortical feeder or a N-cadherin layer as previously described. MGE explants were kept in supplemented *Neurobasal* medium.

For TFM experiment, MGE explants were embedded in 200 µL of 75% *Geltrex* (#12053569, *Gibco*) and cultured on the polyacrylamide (PAA) hydrogels. To ensure that explants were in contact with the PAA hydrogel, they were placed on ice for 10 minutes before being incubated at 37°C for 30 minutes. Then, 3 mL of supplemented *Neurobasal* medium were added. The cultures were maintained at 37°C, 5% CO_2 for at least 24 hours before performing traction force microscopy.

3.2.4. Pharmacological treatment

MGE explants were treated with 1.8 mL 20µM of YAP1 inhibitor TAT-PDHPS1 (#7832/1, *Tocris*) or H_2O (control) diluted in NB. After 24 hours, half of the medium was removed, and treatment was renewed. The dishes were kept at 37°C, 5% CO_2 until the time-lapse imaging.

3.3. BIOCHEMISTRY

3.3.1. Polyacrylamide hydrogels

Polyacrylamide (PAA) hydrogels were polymerized between two surfaces. The holding surface was treated to become hydrophilic, ensuring a strong adhesion of the gel, while the recovering surface was made hydrophobic to enable its easy removal after gel polymerization.

3.3.1.1. *Amino-silanation*

Glass coverslips from *MatTek* dishes (#P35G-0-20-C) were removed and submitted to amino-silanation in order to make them hydrophilic. Amino-silanation was achieved by a 5-minute incubation in 0.1M NaOH, followed by a 5-minute incubation in 0.5 (3-Aminopropyl)-triethoxysilane (APTES, #A3648-100ML, *Sigma-Aldrich*) diluted in 95% isopropanol. The coverslips were then immersed in 2% glutaraldehyde (#354400-500ML, *Merck Millipore*) for 30 minutes. Between each incubations step, the coverslips were rinsed twice with milli-Q water. Once treated, the coverslips were air-dried and stored in the dark until used.

3.3.1.2. *Chloro-silanation*

Plastic film was made hydrophobic through chloro-silanation in order to facilitate its removal from the polymerized gels. The process involved a 5-minute incubation in dichlorodimethylsilane (DCDMS, #440272-100ML, *Sigma-Aldrich*), followed by rinses with distilled water.

3.3.1.3. *Gels preparation*

Polyacrylamide solutions were prepared in order to obtain a stiffness of 1 kPa. The polyacrylamide mixture contained 0.03% N,N'-Methylenebisacrylamide (#M1533-25ML, *Sigma-Aldrich*) and 5% acrylamide (#A4058-100ML, *Sigma-Aldrich*).

Aliquots of 1 mL were filtered through a 0.2 µm filter and subsequently degassed for 30 minutes in order to exhaust the solution of dissolved oxygen. Fluorescent microbeads (FluoSpheres™ carboxylate-modified, 0.1 µm, orange (540/460) #F8800, *Life Technologies Corporation*) were vortexed and sonicated for 30 seconds before being added to the solution (3 µL/mL), followed by the addition 10% ammoniumperoxodisulfate (APS, #9178.3, *Carl Roth GmbH*) and 1% N,N,N,N-tetramethylethylenediamine (TEMED, #T9281-25ML, *Sigma-Aldrich*).

Immediately after gel preparation, 57 µL of solution was added on the chloro-silanated surface, and the amino-silanated coverslip was carefully placed above. The gels were allowed to polymerize for approximately 1 hour in the dark and in inverted position to make sure that the microbeads remained at the hydrogel surface.

Once polymerized, the gels were incubated in DPBS 20 minutes at room temperature covered from light. To prevent hydrogels from cracking, the chloro-silanated plastic sheet was carefully removed from the surface of the gel while keeping them submerged in DPBS. To remove unpolymerized acrylamide, the gels were washed twice for 5 minutes with DPBS.

Then, the gels were functionalized with a 2-hour incubation in hydrazine hydrate (#225819-100ML, *Sigma-Aldrich*), followed by a 1-hour incubation in 5% acetic acid (#15578364, *Fisher Scientific*), both at room temperature. Afterwards, the gels were thoroughly washed three times with DPBS to remove any residual reagents. Afterwards, the gels were stored at 4°C in DPBS to keep them hydrated.

Eventually, the PAA hydrogels were reattached to the *MatTek* dish by applying glue on the outer part of the dish. To ensure sterility of the hydrogels before seeding the MGE explants, the hydrogels were exposed to UV light for 30 minutes while immersed in sterile DPBS.

3.3.2. Western Blotting

3.3.2.1. *Protein lysis*

Cortical cells were washed twice with cold DPBS and lysed with 150 µL of radioimmunoprecipitation assay (RIPA) buffer freshly supplemented with protease (#P8340, *Sigma*), and phosphate (#4906845001, *Sigma*) inhibitor cocktails. Cells were lysed mechanically with a tissue grinder followed by 30 seconds sonication. Proteins were allowed to solubilize on ice for 30 minutes and centrifuged for 10 minutes at 10,000 rpm. Supernatants were transferred to a fresh tube. Protein lysates were then quantified using the *Pierce* BCA Protein Assay Kit (#23223, *ThermoFisher*).

3.3.2.2. *SDS-PAGE and Western Blot*

First, 8% SDS-PAGE gels were prepared to allow protein separation by gel electrophoresis. 40 µg of protein samples were denaturalized by incubating them for 5 minutes at 95°C before

loading them to the gel. A molecular marker (#26619, *ThermoFisher*) was used in order to identify the proteins of interest.

The gel electrophoresis was performed at 120 mV for approximately 1h30 in Running Buffer. Polyvinylidene difluoride (PVDF) membranes (Emersham™ Hybond™ P 0.45 PVDF #10600023, *Cytiva*) were activated with methanol. The transfer was performed at a constant current of 300 mA for 2 hours in Transfer buffer. Membranes were blocked in 5% bovine serum albumin (BSA) diluted in blocking solution (TBS-T) for 1 hour at 4°C.

Then, membranes were incubated overnight at 4°C with the primary antibody (Phospho-Yap1 (Ser127) rabbit #4914911S, *Cell Signaling)* in rotation. The next day, membranes were washed three times for 10 minutes in TBS-T under agitation at room temperature. Then, they were incubated for 45 minutes at room temperature with the secondary antibody (#7074, *Cell Signaling*) at a 1:5,000 dilution in blocking solution. When necessary, membranes were incubated for 2 hours at room temperature with ß-actin-HRP antibody (#12262, *Cell Signaling*) at a 1:10,000 dilution in blocking solution. Finally, the reveal solution (Pierce™ ECL Western Blotting Substrate #32106, *Thermoscientific*) was added to the membranes before proceeding to detection with *Amersham ImageQuant™ 800* western blot imaging system (*Cytiva*). When necessary, membranes were washed in stripping buffer followed by two washes in PBS and two washes in TBS-T. Afterwards, the membranes were ready for blocking and antibody incubation. Information concerning the composition of the solutions used for this experiment can be found in supplementary figures.

3.3.3. Immunofluorescence

Immunofluorescence staining against GFP was performed exclusively on reference glass slides. First, antigen retrieval was carried out by immersing the slides in a 1X Target Retrieval Solution (#S1699, *Dako*), and heating them at 126°C for 11 minutes under 1.4 bar pressure. The slides were then cooled to room temperature for 20 minutes in the same solution before being washed twice for 2 minutes with milli-Q water.

Secondly, the nonspecific sites were blocked by incubating the slides for 1 hour at room temperature in a 1X dilution of Animal-Free Blocking solution (#15019L, *Cell signaling*). The

primary anti-GFP antibody (goat polyclonal, #ab6673, *Abcam*) was diluted at 1:500 in Real-Antibody-Solution (#S2022, *Dako*) and incubated overnight at 4°C.

The following day, slides were washed three times for 5 minutes in PBS. The secondary antibody (#A11055, *ThermoFisher*) was diluted (1:1,000) in PBS and incubated for 1 hour at room temperature. Nuclear staining was performed by incubating the slides in a 1:10,000 dilution of DAPI (1mg/mL DAPI, #D9542, *Sigma-Aldrich*) for 5 minutes at room temperature, followed by three washes of 5 minutes in PBS.

Finally, the slides were mounted in fluorescence mounting medium (S3023, *Dako*) and dried in the dark at room temperature before being stored at 4°C. Image acquisition was performed by *GIGA Imaging Platform* with the slide scanner (*ZEISS Axioscan 7*).

3.4. LASER MICRODISSECTION

3.4.1. Tissue preparation

Embryonic heads from six E13.5 and six E16.5 embryos were fixed in 4% paraformaldehyde (PFA, #15710, *Electron Microscopy Science*) overnight at 4°C and subsequently stored in 70% ethanol at 4°C until paraffin embedding, which was performed by the *Histology Platform*.

Coronal sections of 5µm were prepared using a microtome (*Leica RM2145*). Two slices per embryo head were mounted on standard glass slides to serve as reference slides for visualizing Dlx5,6-Cre:GFP-positive interneurons and their migratory pathways. Additionally, five slices were placed on PEN membrane slides (#11600288 *Leica Microsystems, ThermoFisher*) to allow laser microdissection experiment. Before proceeding to downstream analysis (*i.e.* immunofluorescence on glass slides and laser microdissection on PEN slides), deparaffination was performed following serial washes in isopropanol baths of decreasing concentrations. Throughout the whole protocol, HPLC water (#23595.400, *VWR chemicals*) was used.

3.4.2. Laser capture microdissection

Laser microdissection of the two brain regions of interest was performed using the *Leica LMD 7000* system. For each piece of tissue, an oval-shaped area of approximately 3,300 μm^2 was excised with a 63X magnification. The dissected tissue was collected in the cap of 0.6 mL

Microcentrifuge tube (MCT-060-L-C, *Corning*), and were subsequently visualized with a 10X magnification. Then, they were transferred to PMMA tubes.

	Power	Aperture	Speed	Offset	Specimen Balance	Head Current	Pulse Frequency
E13.5	25	4	6	25	1	119	70
E16.5	30	3	6	67	14	100	637

Table 1*: Leica laser microdissector settings for E13.5 and E16.5 brain tissues.*

Since 5 brains per developmental stage were processed, a total of 25 CP samples and 25 IZ samples were collected per stage. Prior to analysis by the chemistry laboratory (*Uliège*), all samples were stored at 4°C.

3.4.3. LC-MS/MS analysis

Samples were collected and centrifuged at 16 000 g for 10 minutes. Afterwards, samples were prepared for mass spectrometry analysis by the *Chemistry Laboratory of Uliège*.

Briefly, citric acid was added to each sample for antigen retrieval during a 1-hour incubation at 99°C. During this incubation, the samples were centrifuged every 10 minutes at 15 000 g for 1 minute. Next, bicarbonate was added to serve as pH buffer, and dithiothreitol (DTT, #J15397 *ThermoFisher Scientific*) to dissolve the disulfuric binds and denaturate the proteins. The samples were incubated at 56°C for 40 minutes. To complete denaturation process, iodoacetamide (IAA, #I1149-5g *Sigma-Aldrich*) was added to ensure alkylation of disrupted disulfuric bridges, and the samples were left 30 minutes in the dark. Finally, trypsin solution also containing n-Dodecyl-β-D-maltoside (DDM, D5172-1g *Sigma-Aldrich*) was added and the samples were kept overnight at 37°C. The next day, trypsin activity was stopped using trifluoroacetic acid (TFA).

Samples were consequently ready to be analyzed by the mass spectrometer (timsTOF SCP, *Bruker*).

3.5. TIME LAPSE

3.5.1. Imaging

Time lapse was performed 48 hours after the first pharmacological treatment (control or TAT-PDHPS1), using *Nikon A1R* microscope. Several positions were selected to observe the migration of interneurons from MGE explants in both conditions. For each movie, pictures every 2 µm (10 to 13 Z) were taken every 5 minutes for 5 hours, with 20X objective. The whole experiment was conducted under controlled conditions, with a temperature of 37°C and 5% CO_2.

3.5.2. Data analysis

Time lapse images were visualized and analyzed with *Fiji* (*ImageJ*). *StackReg* plugin was used to align images and eliminate objective drift, and *MtrackJ* plugin was used to track soma movements of migrating Dlx5,6-Cre:GFP-positive neurons. Approximately 10 migrating cells per time lapse were included in the analysis of data.

Several parameters were used to quantify the neuronal migration: the total duration of measurements (5 hours), the net distance of displacement (in microns), and the total path length of the neuron during migration (in microns).

Nucleokinesis events were defined as timepoints showing a displacement amplitude superior than or equal to 5 microns. Based on these data, the average amplitude (in microns), the total number of nucleokinesis and their frequency (number of events per hour) were calculated. In contrast, the number and time of pausing periods was also determined from amplitude values equal to 0 microns.

3.6. TRACTION FORCE MICROSCOPY

3.6.1. Imaging

Traction force microscopy was performed using an epifluorescent microscope (*Apotome Zeiss*) at the *GIGA Imaging Platform*.

Before conducting the traction force microscopy measurements, we recorded a time-lapse of migrating neurons, capturing images every 30 seconds over a period of 30 minutes. Neurons

were selected based on their proximity to the fluorescent beads, ensuring they were maximum 10 µm far, which is necessary for measuring the effects of the migration forces applied by the interneuron.

For each selected neuron, we acquired two set of images at 40X magnification (40x-water immersion objective): one of the fluorescent microbeads in RFP (AF568) channel, and another of the neurons in GFP (AF488) channel.

To remove the cells, 1 mL of ethylenediaminetetraacetic acid (EDTA, #E5124-500G, *Sigma-Aldrich*) and 400 µL of 10% SDS (#8029.3, *Carl Roth GmbH*) were applied. After a 10-minute incubation to ensure cell death and detachment, the solution was removed, the hydrogel was rinsed with 2 mL of PBS and incubated with conditioned media for 20 minutes, in order to allow the gel to relax and recover its mechanical properties.

Next, Z-stacks images of the fluorescent beads were acquired, with 10 images taken at 1 µm intervals. To ensure consistency in focal planes between the initial and post-relaxation images, reference points from the first images set were used.

The whole experiment was conducted under controlled conditions, with a temperature of 37°C and 5% CO_2.

3.6.2. Data analysis

Analyses from three cINs were conducted at two specific time points: T0 and T1 (30 minutes after T0), in order to capture dynamic changes in traction forces during migration. Six images were analyzed using *FIJI* (*Image J*): three phase-contrast images showing the position of cINs, and three corresponding fluorescent images representing the microbeads within the polyacrylamide gel.

First, low-resolution images (1500 x 1281 pixels, 8-bit) were processed using a *FIJI* macro to prepare and align the image stacks. To determine bead displacement, a reference image focusing on microbeads was acquired after removal of the cells, corresponding to initial beads disposition, with no external influences.
The shift between beads reference position and displaced position was aligned using the *Template Matching* plugin in *FIJI*.

Then, the Particle Image Velocimetry (PIV) – *Iterative PIV Basic* plugin was used to measure and show beads displacement vectors. Post-processing included a normalized median test, and replacement of invalid vectors with local medians.

To convert bead displacement into traction forces, *Fourier Transform Traction Cytometry* (FTTC) was applied using the FTTC plugin for FIJI. The following parameters were used:

- Pix size: 0.208 µm/pixel
- Poisson's ratio: 0.5
- Young's modulus of the hydrogel: 1 kPa

FTTC outputs provided vector maps of traction forces exerted by individual neurons. These values were subsequently exported and plotted using *MATLAB*. Force heatmaps show the spatial distribution and intensity of traction forces around the cell body and leading processes.

3.7. STATISTIC ANALYSES

Statistical analyses were performed using GraphPad Prism 8. Data are presented using mean ± standard error of the mean (SEM). Comparisons were made between two conditions: control and experimental treatment, and *Student's t-tests* were applied.
In some experiments, statistical comparisons were performed on datasets with $n < 3$, in which cases preliminary results are shown for illustrative purposes. A p-value < 0.05 was considered statistically significant.

RESULTS

4. RESULTS

4.1. Yap/Taz pathway regulates the migration of cortical interneurons

4.1.1. Pharmacological inhibitor TAT-PDHPS1 increases phosphorylation of Yap/Taz in cortical interneurons

At a cellular level, E13.5 and E16.5 cINs display distinct migration dynamics.[68] In addition, Yap1 is downregulated in Dlx5,6-Cre:GFP cINs through the development (data not shown), positioning it as an interesting mechanotransduction candidate. To understand the role of Yap1 in the migration process of cINs, we treated E13.5 MGE explants with the pharmacological inhibitor TAT-PDHPS1. This drug is a combination of the cell-penetrating peptide sequence TAT, and the endogenous peptide PDHPS1. By binding to PTPA, PDHPS1 affects its ability to activate PP2A. In the Hippo pathway, PP2A dephosphorylates both transcriptional coactivators Yap1 and Taz, enabling their nuclear translocation and transcriptional activity. Consequently, the intracellular cascade initiated by PDHPS1 leads to persistent phosphorylation of Yap/Taz, ultimately causing their cytoplasmic retention. [69]

In order to evaluate the efficacy of TAT-PDHPS1 drug in cultured cortical cells, we examined the levels of phosphorylated (Ser127) and total-Yap1 after 48 hours of drug treatment. Western blot analysis using phosphorylated-Yap1 (pYap1) antibody allowed us to identify both pYap1 (75 kDa) and phosphorylated-Taz (pTaz, 50 kDa) (***Fig 5A***). Interestingly, TAT-PDHPS1 treatment induces an increase of both proteins in their phosphorylated state, with a 1.8 fold change in pYap1 and more than 3 fold change in pTaz (***Fig. 5B***).
Analyses of total-Yap1 revealed a decrease in levels under TAT-PDHPS1 treatment (***Fig. 5C***), with a 2 fold change compared to control conditions (***Fig 5D***).

These preliminary results indicate that TAT-PDHPS1 treatment inhibits Yap1 in cortical neurons.

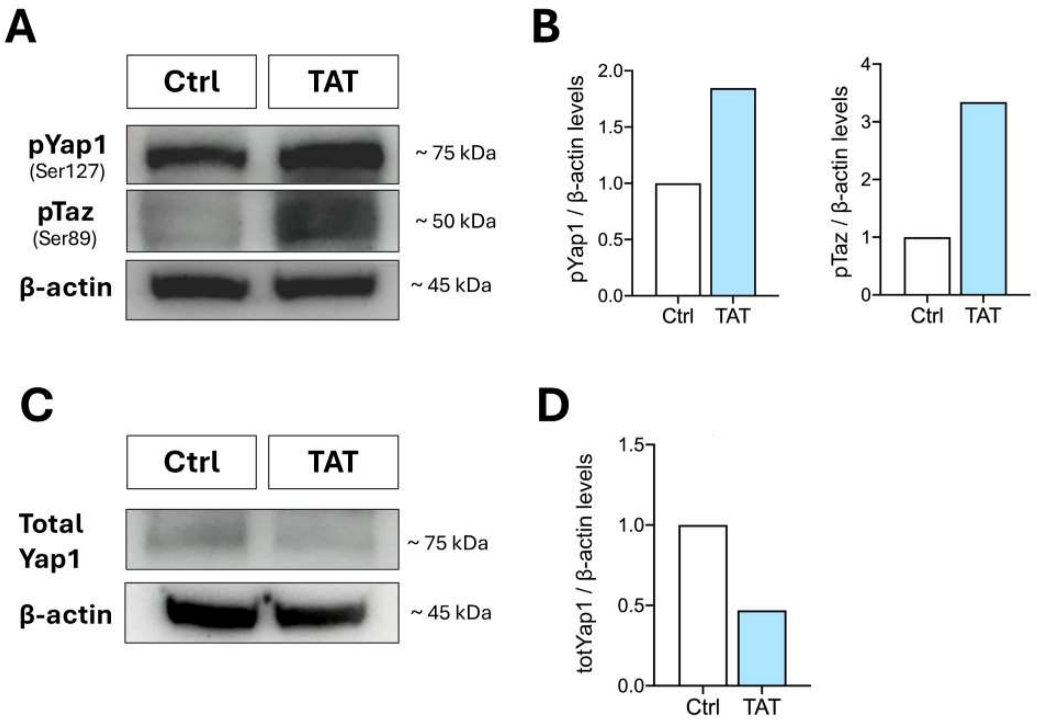

Figure 5: ***Western Blot analyses of Yap1 and Taz proteins when exposed to TAT-PDHPS1 treatment***.

A) *Western Blot bands of phosphorylated Yap1 (pYap1), phosphorylated Taz (pTaz) (bin 5x5, 1min), and β-actin as a loading control. Protein levels were analyzed in control (Ctrl) conditions and in treated condition with TAT-PDHPS1 (TAT).* ***B)*** *Quantifications of phosphorylated Yap (pYap) and phosphorylated Taz (pTaz) levels normalized to β-actin. The values represent the fold change relative to control condition (Ctrl), which was set to 1.* ***C)*** *Western blot bands of total Yap1 and β-actin as a loading control. Protein levels were analyzed in control (Ctrl) conditions and in treated conditions with TAT-PDHPS1 (TAT).* ***D)*** *Quantification of total Yap1 (totYap1) levels normalized to β-actin. The values represent the fold change relative to control condition (Ctrl), which was set to 1.* *N = 1*

4.1.2. YAP/TAZ activity regulates cortical interneuron migration

To investigate the effects of Yap1 inhibition on the migration of cortical interneurons, we performed live-imaging of E13.5 Dlx5,6-Cre:GFP-positive MGE-derived cINs that were previously treated with the TAT-PDHPS1 peptide (***Fig. 6A***).

Time-lapse analysis indicates that inhibition of Yap1 leads to slower migration (***Fig. 6B***), reduced frequency of nucleokinesis (***Fig. 6C***) and increased pausing time (***Fig. 6D***) compared to control. However, the amplitude of nucleokinesis remained unchanged (***Fig. 6E***).

These results suggest that Yap/Taz modulate the migration of cortical interneurons. However, in this model, the MGE-derived interneurons are migrating on a homochronic cortical feeder. Therefore, we could not exclude the possibility that the observed effect was partly due to inhibition of Yap/Taz in the cortical cells.

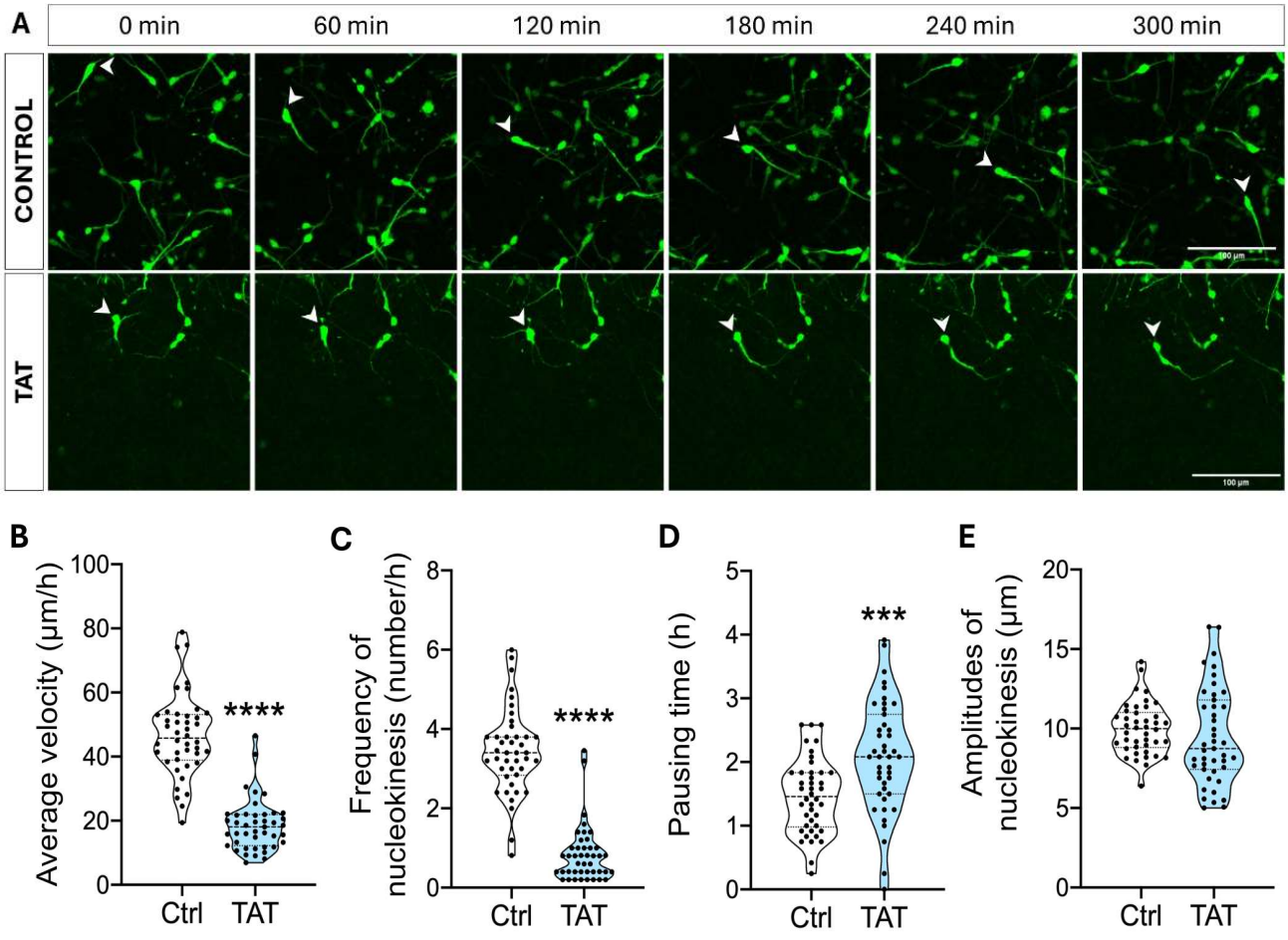

***Figure 6*: E13.5 cortical interneurons migratory behavior under TAT-PHDPS1 treatment.**

A) *Time lapse pictures of migrating Dlx5,6-Cre:GFP-positive cortical interneurons under control condition (H2O) or experimental condition (TAT-PDHPS1). Pictures were acquired with Nikon A1R microscope.* ***B)*** *Violin plot showing average velocity (µm/h) of control cINs and cINs treated with TAT-PDHPS1. This parameter was calculated by dividing the total net distance (hours) by the total duration of time lapse (hours).* ***C)*** *Violin plot showing nucleokinesis frequency (number/h) in control cINs and in cINs treated with TAT-PDHPS1. This parameter was calculated by dividing the number of nucleokinesis by the total duration of time lapse (hours).* ***D)*** *Violin plot showing pausing time (h) in control cINs and in cINs treated with TAT-PDHPS1. This parameter was calculated by dividing the number of pauses (number of amplitude values equal to 0 µm) by 12.* ***E)*** *Violin plot showing average amplitudes of nucleokinesis (µm) in control cINs and in cINs treated with control. This parameter was measured using MtrackJ plugin in FIJI (Image J). N = 4 embryos, n = 42-43 neurons.*

Consequently, to prove a direct effect of Yap1 on the migration of MGE-derived interneurons, we cultured MGE explants from E13.5 embryos on an acellular model consisting of N-cadherin / fibronectin coating (***Fig. 7A***). The migrating area of Dlx5,6-Cre:GFP-positive interneurons from the MGE explant was calculated using *FIJI* (*Image J*) and was normalized to the explant size. Preliminary results indicate that the migrating area of Dlx5,6-Cre:GFP-positive MGE cells on acellular coating in treated conditions was significantly decreased compared to control conditions (***Fig. 7B, C***). Taken together, these results suggest that Yap/Taz pathway directly regulates the migration of E13.5 cortical interneurons.

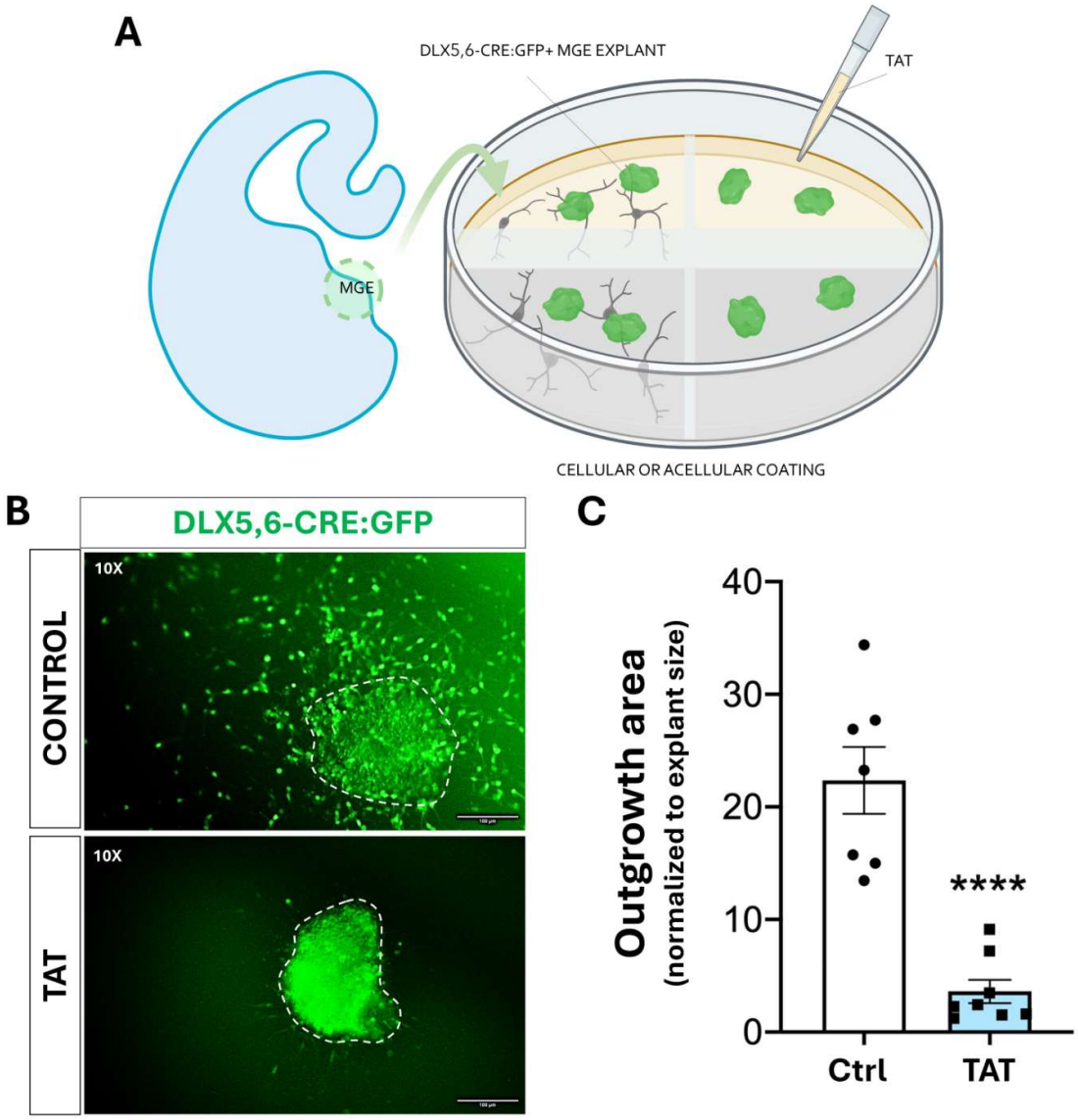

***Figure 7**: **E13.5 cortical interneuron migration upon TAT-PDHPS1 treatment in an acellular model**. **A)** Schematic representation of a coronal section from mouse embryo left hemisphere, showing the medial ganglionic eminence (MGE). Explants of Dlx5,6-Cre:GFP-positive MGE were seeded and maintained in culture on the cellular or acellular model, and treated with vehicle (H_2O) or TAT-PDHPS1. **B)** Pictures of E13.5 MGE explants and migrating Dlx5,6-Cre:GFP-positive cINs in control and treated condition, on acellular coating model. The MGE explant is highlighted on both pictures, and the migrating area was calculated from the delimited explant zone. Pictures were captured with an inverted microscope, using magnification 10X. **C)** Graph of migrating area of Dlx5,6-Cre:GFP-positive cINs from MGE explant, previously seeded on an N-cadherin coating and treated either with vehicle (H_2O) TAT-PDHPS1 (TAT). The outgrowth area was normalized to the size of the MGE explant. Graph represents mean ± SEM, P-value < 0.0001 (****), N =1 embryo per condition.*

4.2. Embryonic cortical interneurons display traction forces

Yap/Taz is a potential mechanotransducer in migrating cortical interneurons. It has been shown that Yap1 senses and transduces to mechanical signals from the ECM through its close interaction with the actin cytoskeleton.[70] Given its potential role in the modulation of forces during neuronal migration, we sought to investigate the traction forces applied by the cytoskeleton of migrating cINs. To this aim, traction force microscopy was performed on E13.5 MGE explants cultured on a 1 kPa polyacrylamide hydrogel (***Fig. 8A***).

Three cINs were selected for analyzes, and pictures of both cIN and fluorescent beads were taken. This approach allowed us to overlay the position of microbeads before and after removal of the cells (***Fig. 8B, C***). Pictures were analyzed at two distinct time points; T0 and T1. Plus, at T0, we observe that cIN morphology exhibits a branched leading neurite, in opposition to T1 (***Fig. 8B, C***).

In order to visualize the movement of microbeads, analyses were performed using *FIJI* (*Image J*) and generated a particle image velocimetry (PIV) output, representing the vector of displacement of the microbeads at timepoints T0 and T1. Higher density and magnitude of vectors are observed around the interneuron at T0, with a specific concentration around the axonal growth cone and the nucleus (***Fig. 8D***). At T1, the displacement vectors are less intense, although the main areas of movement remain concentrated in the same regions (***Fig. 8E***).

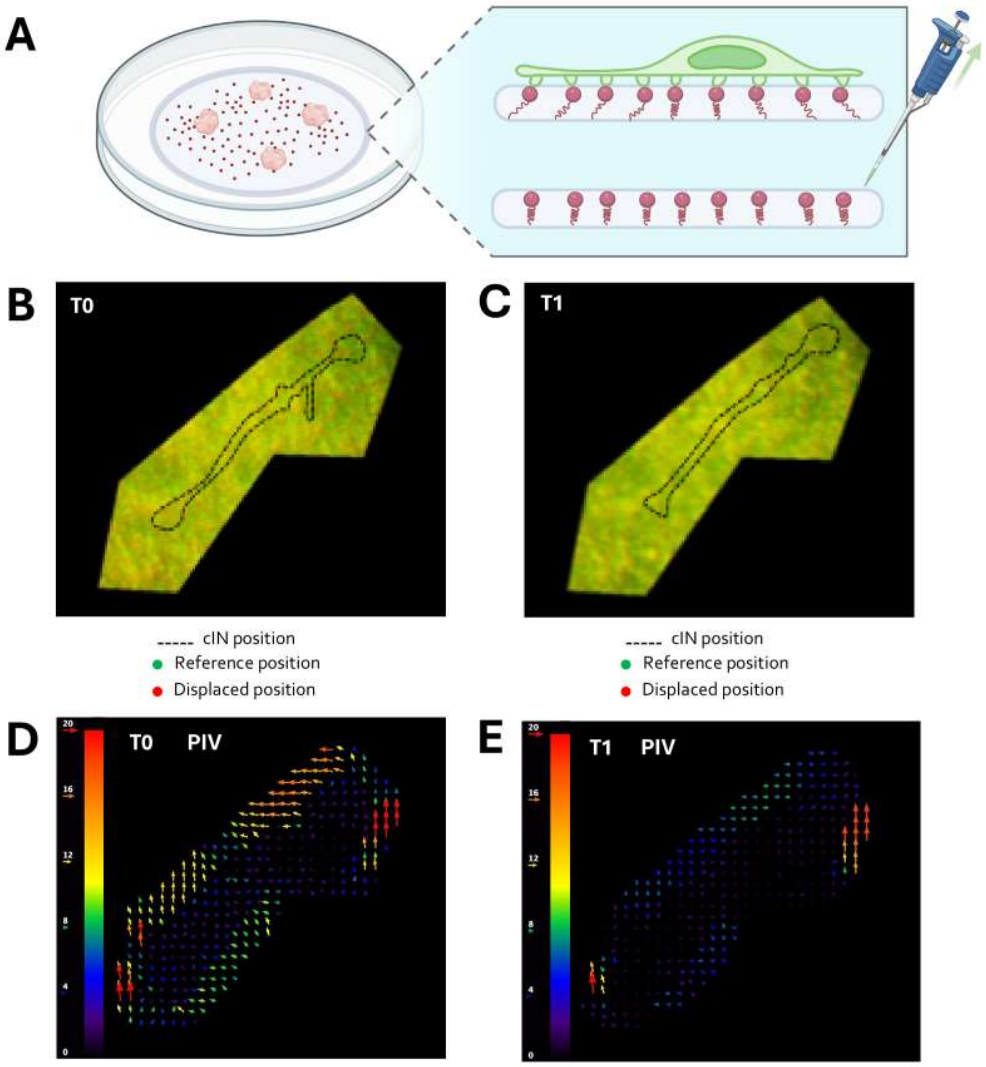

Figure 8*: Characterization of microbeads displacement within the hydrogel under E13.5 cortical interneuron traction forces.** ***A) *Representation of polyacrylamide hydrogels. Medial ganglionic eminence (MGE) explants from E13.5 or E16.5 mouse embryos are seeded on 1 kPa PAA hydrogels, whose surface contains fluorescent microbeads. Migrating cINs from MGE explants perturb the microbeads disposition. Once the cells are lysed and removed from the culture, the hydrogel is able to relax and the microbeads return to their initial position. This figure was created with BioRender.* ***B)*** *Cropped picture of the hydrogel with a representation of the cortical interneuron position at T0. Microbeads represented in green demonstrate their initial position when the hydrogel is relaxed, after the removal of the cells. Microbeads represented in red demonstrate their displaced position, due to the forces applied by the migrating cortical interneuron.* ***C)*** *Cropped picture of the hydrogel with a representation of the cIN position at T1. The same system is used to demonstrate microbeads position.* ***D)*** *Particle Image Velocimetry (PIV) at T0. PIV output represents the displacement of fluorescent microbeads in the gel between the deformed state (when the cell is present) and the relaxed state (after removal of the cell). Each arrow shows the direction and the intensity of beads displacement and vary from 0 to 20 µm.* ***E)*** *Particle Image Velocimetry (PIV) at T1.*

Next, we applied *Fourier Transform Traction Cytometry* (FTTC) to estimate the traction forces exerted by cINs on the substrate. This mathematical model takes into account the hydrogel stiffness (*i.e. 1000 Pa*) to generate force field maps at both timepoints. The arrows represent the orientation and intensity of force vectors that are applied by the migrating interneurons on the microbeads composing the hydrogel. As observed previously, most of the forces generated by the cIN are located around the axonal growth cone and around the nucleus (***Fig. 9A, B***). At T0, traction forces are notably more intense, especially at the growth cone (***Fig. 9A***). At T1, even though forces appear globally reduced, we still observe a concentration of forces around the growth cone (***Fig. 9B***). This is consistent with the morphology differences observed between both timepoints; dynamic branching increases the forces detected around the leading process.

Complementary heatmaps were generated using *MATLAB* software, which also highlight stronger zones of tension at T0 compared to T1 (***Fig. 9C, D***). The differences of bead displacement and neuronal forces between both timepoints indicates that the intrinsic traction forces displayed by cINs are dynamic and transient during time.

Since our previous results suggest that the generation of traction forces is a dynamic process, we calculated the distribution of force magnitude from three independent interneurons at T0 and T1 (***Fig. 9E***). Consistent with previous studies, the average of stress generated by migrating cINs remain below 50 Pa (***Fig. 9E, F***).[71] A small proportion of forces ranges between 50 and 250 Pa, consistent with localized peaks of higher traction observed around the growth cone in the previous figures (***Fig. 9A, D***).

Taken together, these data suggest that migrating cINs exert dynamic traction forces of an average of 10 Pa, and that the stronger forces are particularly displayed around the nucleus and by the axonal growth cone. Increased force magnitudes are typically generated by cINs that are exploring and sensing their environment., compared to inactive non-branching cells. This suggests that the exploratory behavior of branching interneurons can be associated with amplified intrinsic traction forces generation.

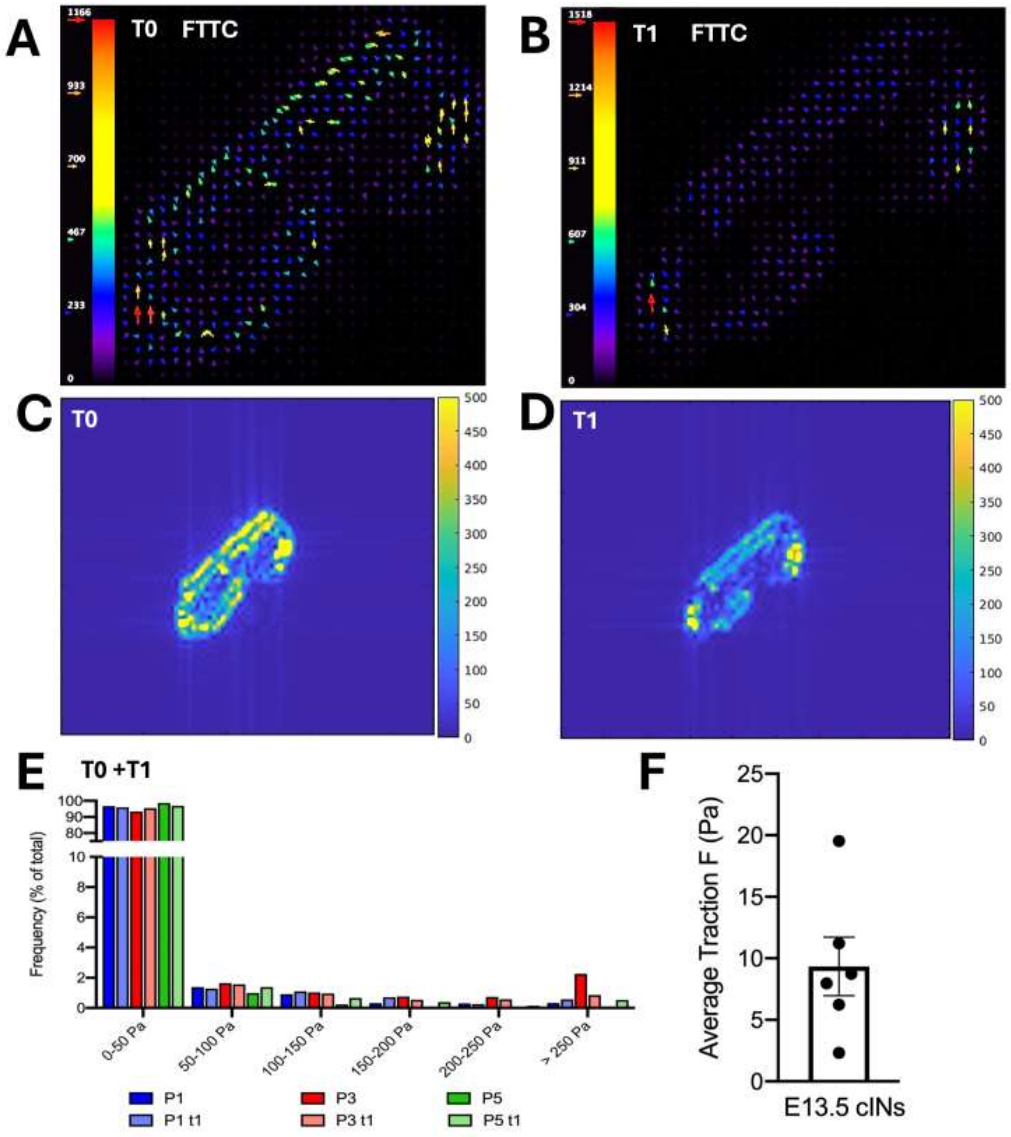

Figure 9: ***Characterization of traction forces applied by E13.5 cortical interneurons.*** ***A)*** *Fourier Transform Traction Cytometry (FTTC) generated with FIJI: force field map displaying vectors of traction forces applied by the cIN on the hydrogel, at T0. Forces vary from 0 to 1200 Pa.* ***B)*** *Fourier Transform Traction Cytometry (FTTC) generated with FIJI: force field map displaying vectors of tractions forces applied by the cIN on the hydrogel, at T1. Forces vary from 0 to 1500 Pa.* ***C)*** *Heatmap of magnitude showing the spatial distribution of forces around the interneuron and their magnitude ranges at T0.* ***D)*** *Heatmap of magnitude showing the spatial distribution of forces around the cIN and their magnitude ranges at T1.* ***E)*** *Histogram showing the distribution of forces into different ranges of values and their frequency for the three analyzed cINs at T0 and at T1.* ***F)*** *Bar plot with individual data points showing the average traction forces (Pa) applied by the migrating E13.5 cIN.* *n = 3 neurons per time point, N = 1 embryo.*

4.3. Expression of ECM proteins differs between neocortical regions and at different developmental stages

Embryonic mouse cortical tissue stiffens as the brain development takes place.[41] In addition, previous data from our laboratory detected differences in the migration dynamics of cINs in the two migration streams (*i.e.* the CP and the SVZ/IZ) during development (data not shown). In order to better understand the extracellular environment where cINs migrate and to investigate their interactions with ECM, we laser microdissected the two migratory streams of cINs and analyzed the samples with mass spectrometry (***Fig. 10A***).

In order to visualize the migration streams of Dlx5,6-Cre:GFP-positive cINs in brain coronal section slices, reference slides of both stages were prepared and immunofluorescence against GFP was performed. The results show interneurons entering the cortex through the two streams, located in the IZ and the CP, at E13.5 (***Fig. 10B***). At E16.5, we observe that, in addition to the two tangential streams of migration, cINs also diffuse within the distinct areas of the developing cortex, with visible migrating cells from the SVZ/IZ to the CP (***Fig. 10C***).

Afterwards, coronal section slices of E13.5 and E16.5 embryo heads were prepared on PEN slides, and laser microdissection of both regions of interest (*i.e.* CP and SVZ/IZ) was performed (***Fig. 11A***). Each piece of tissue was collected in the cap of an *Eppendorf* tube (***Fig. 11B***). Microdissected tissue samples were sent to mass spectrometry laboratory in order to compare the proteomic content of CP and SVZ/IZ.

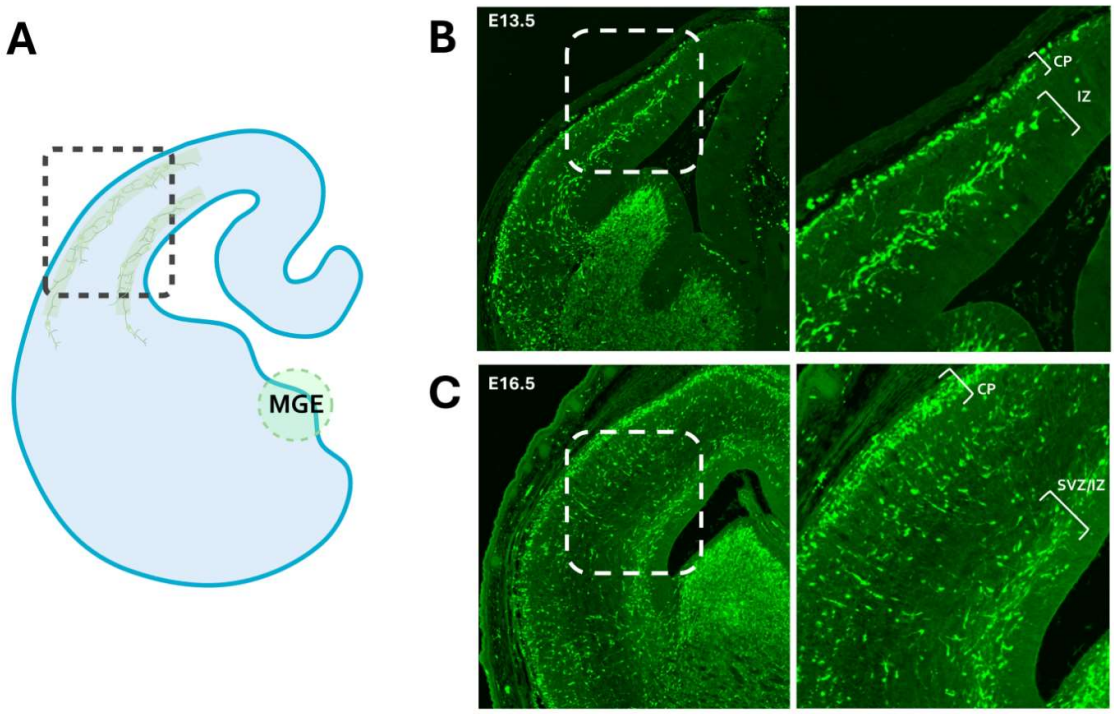

Figure 10: ***Visualization of cINs migratory pathways in neocortex at E13.5 and E16.5.*** ***A)*** *Schematic representation of a coronal section from left hemisphere of mouse embryo, highlighting the medial ganglionic eminence (MGE), and the migratory streams of cINs in the cortical plate (CP) and the intermediate zone (SVZ/IZ). This illustration was created with BioRender.* ***B)*** *Immunofluorescence image of E13.5 coronal section from mouse embryo head, focused on the left hemisphere, then showing the CP and SVZ/IZ regions. GFP-positive cells (green) correspond to Dlx5,6-Cre:GFP-positive neurons. Images were acquired with ZEISS Axioscan 7.* ***C)*** *Immunofluorescence image of E16.5 coronal section from mouse embryo head, focused on the left hemisphere, then showing the CP and SVZ/IZ regions. GFP-positive cells (green) correspond to Dlx5,6-Cre:GFP-positive neurons. Images were acquired with ZEISS Axioscan 7.*

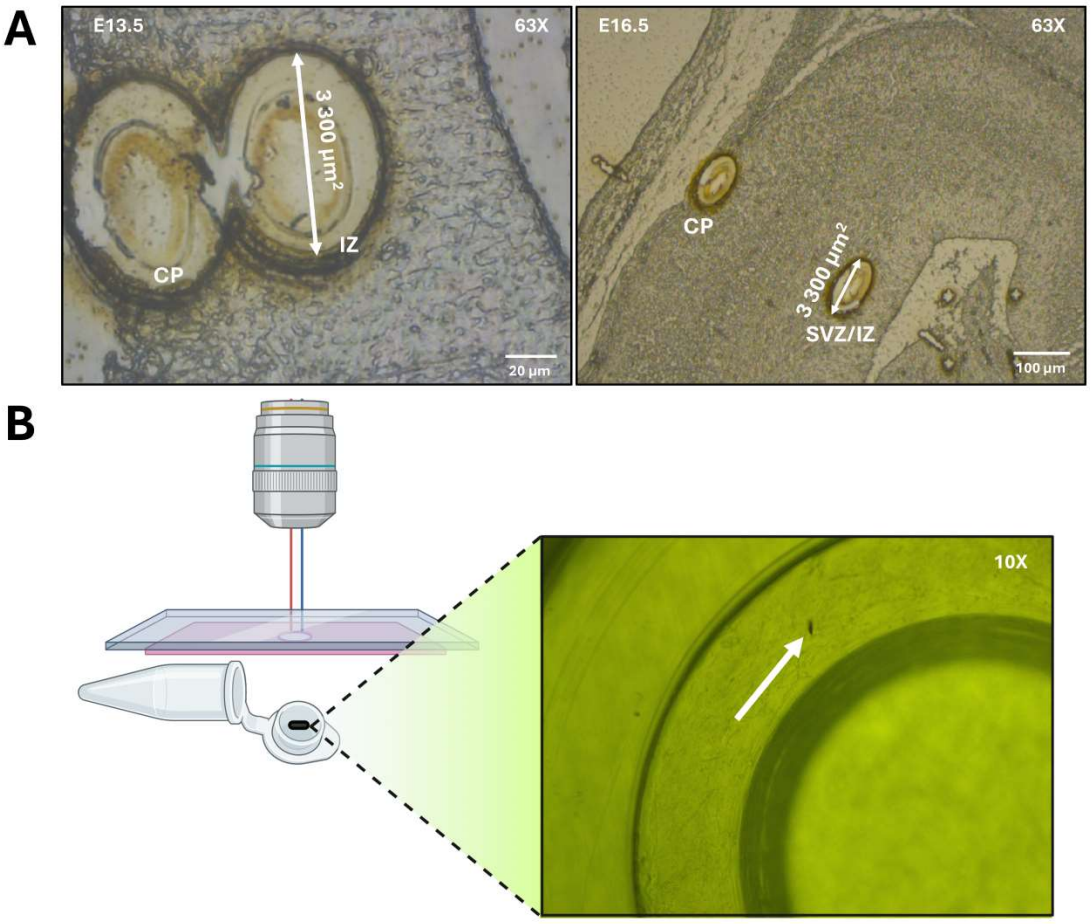

Figure 11: ***Laser microdissection of neocortical zones of interest.*** ***A)*** *Pictures showing coronal sections from left hemisphere of E13.5 and E16.5 brain embryos. On both developmental stages, CP and SVZ/IZ were laser microdissected. The cut area was 3,300 µm². Pictures were taken with Leica laser microdissector 7000, 63X magnification.* ***B)*** *Picture representing microdissected tissue in the cap of an Eppendorf tube. Collected sample is indicated by the arrow. Figure was designed with BioRender, and picture was acquired with Leica laser microdissector 7000, 10X magnification.*

The mass spectrometry analysis detected more proteins at E13.5 (31.4%) than at E16.5 (16%). The comparison between all identified proteins – including intracellular proteins and ECM proteins – at E13.5 and E16.5 indicates that approximately 50% of all proteins are common at both stages (***Suppl. Fig. 1***).

As the neocortex undergoes intense remodeling between E13.5 and E16.5, we focus on the ECM proteome to investigate stage-specific features as well as conserved processes that may support key development events, such as cell migration, ECM-cell signaling, and tissue structuring. To distinguish ECM components from intracellular proteins, a reference database of ECM mouse-specific proteins was established, including GO-term lists related to the mouse extracellular matrix (***Suppl. Table 2***), in combination with data from *Mus musculus Matrisome Project*. Datasets of all detected proteins were intersected with this reference dataset in order to highlight ECM-related proteins.

More than 60% of ECM-related proteins detected in our samples were common to both stages (***Fig. 12A***). Functional enrichment analyses of ECM-related proteins common to both E13.5 and E16.5 datasets highlighted common functions that are conserved across both stages, potentially reflecting core mechanisms involved in cortical development (***Fig. 12B***).
The strongest enrichment was detected for ***myelin sheath*** and ***collagen-containing ECM*** GO-terms, which may reflect early presence of structural or scaffolding precursor components involved in axonal development in the neocortex at both stages. Furthermore, the analysis revealed an enrichment of ***cytoskeletal protein binding***, ***actin filament binding***, ***signaling receptor binding***, ***calcium-dependent protein binding***, and a ***positive regulation of cell migration***. These GO-terms are directly linked to cell migration and mechanotransduction processes. The presence of proteins associated with the ***distal axon*** also supports the involvement of growth cone during both stages.
Additional GO-terms related to ***protein folding***, ***response to stress***, ***smooth endoplasmic reticulum*** and ***vesicles*** point toward a sustained intracellular activity, in particular protein synthesis, processing and secretion – potentially contributing to ECM remodeling.
Altogether, functional enrichment analysis indicates that cell-ECM interactions and communication, notably involved in cell survival and migration, are maintained across both stages.

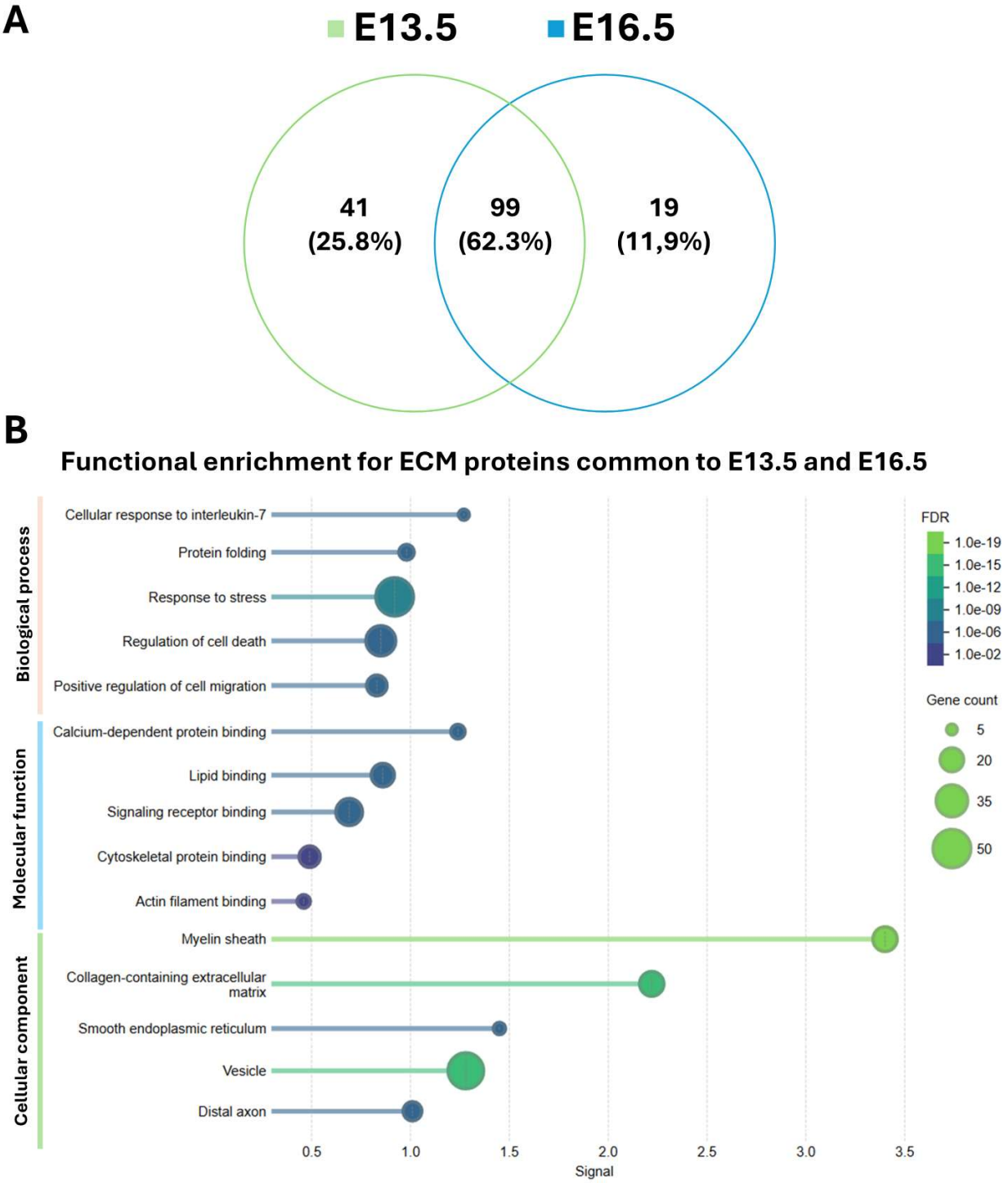

Figure 12: ***Violin plot and functional enrichment analyses.*** ***A)*** *Violin plot comparing database of all proteins detected at E13.5 (green) with database of all proteins detected at E16.5 (blue).* ***B)*** *Functional enrichment for ECM proteins that were detected at E13.5 and E16.5. Functional enrichment regroups proteins into GO-term lists that are sorted according to signal, gene count, and false discovery rate (FDR). The five most relevant GO-terms from three categories (i.e. biological process, molecular function, cellular component) are represented on the enrichment visualization, and sorted according to signal measures. Gene count indicates how many proteins from the network are annotated to the GO-term. FDR values are described using a color code, and indicate how significant the enrichment is.* *N = 5 E13.5 embryos, 1 E16.5 embryo.*

Approximately 25% of ECM-related proteins were exclusively detected at E13.5 (***Fig. 12A***). Functional enrichment analysis on this E13.5 unique dataset revealed enrichment of lots of GO-terms associated with ***focal adhesions***, indicating numerous interactions and active communication between cells and their surrounding ECM (***Suppl. Fig. 2***).

Interestingly, the enrichment of proteins associated with ***filopodia*** suggests the presence of molecular components related to the leading edge of migrating cells within the E13.5 neocortical ECM.

Furthermore, the detection of ***collagen***, ***calcium-dependent***, and ***signaling receptor-binding proteins*** in both the E13.5-exclusive and E13.5/E16.5-common datasets suggests that these functional categories are consistently present, yet with a stage-specific diversity of proteins.

Only ~12% of ECM-related proteins were exclusive to E16.5 (***Fig. 12A***). Due to the small size of this dataset, the *STRING* interaction network did not present significantly more interactions than expected in a random set of proteins.

However, functional enrichment revealed significant FDR values for few GO-terms (data not shown), particularly "***extracellular exosome***" and "***collagen-containing extracellular matrix***", suggesting a molecular signature enriched in components related to extracellular vesicles and collagen in the E16.5 neocortical ECM.

At E13.5, developmental stage, most of cINs are still transiting in the IZ and have not reached the CP yet. Therefore, we concentrate on the ECM-proteins that were detected exclusively in the IZ, and those common to both zones at E13.5 (***Fig. 13A***).

Within our dataset of ECM-proteins detected at E13.5, 30% were exclusively detected in SVZ/IZ, while 52% of proteins were unique to CP (***Fig. 13B***). Around 60% of proteins were common to both cortical regions, suggesting an homogenous expression throughout the cortex.

The functional enrichment analyses of IZ neocortical region at E13.5 highlights an environment where ECM changes and cell-ECM interactions take place (***Fig. 13B***). Indeed, GO-terms such as ***regulation of ECM assembly*** and ***regulation of proteolysis*** describe an active remodulation of ECM. Plus, ***regulation of cell-substrate adhesion***, ***regulation of focal adhesion assembly***, ***integrin and collagen binding***, and ***cell adhesion binding*** demonstrate that dynamic adhesion structures are formed. Of interest, the resulting enriched processes are necessary for cell-ECM interaction and to support neuronal migration.

Plus, ***positive regulation of exocytosis*** and ***vesicle*** GO-terms indicate a secretion of ECM proteins or enzymes that might be involved in the remodelling. This suggests that, beyond responding to external cues, cells may also actively participate in the environment remodeling through synthesis and secretion of ECM-related components.

Neurons undergo changes in their cytoskeleton in response to mechanical signals. Those signals are sensed through focal adhesions and integrins, which are later transduced via calcium-dependent intracellular signaling pathway. In this regard, GO-terms for molecular functions include: ***calcium-depend protein binding***, ***cortical microtubule cytoskeleton***, ***cell basal cortex***, and ***focal adhesion*** terms, reinforcing the idea that E13.5 cells migrating in IZ are sensitive to external signals and adapt in response.

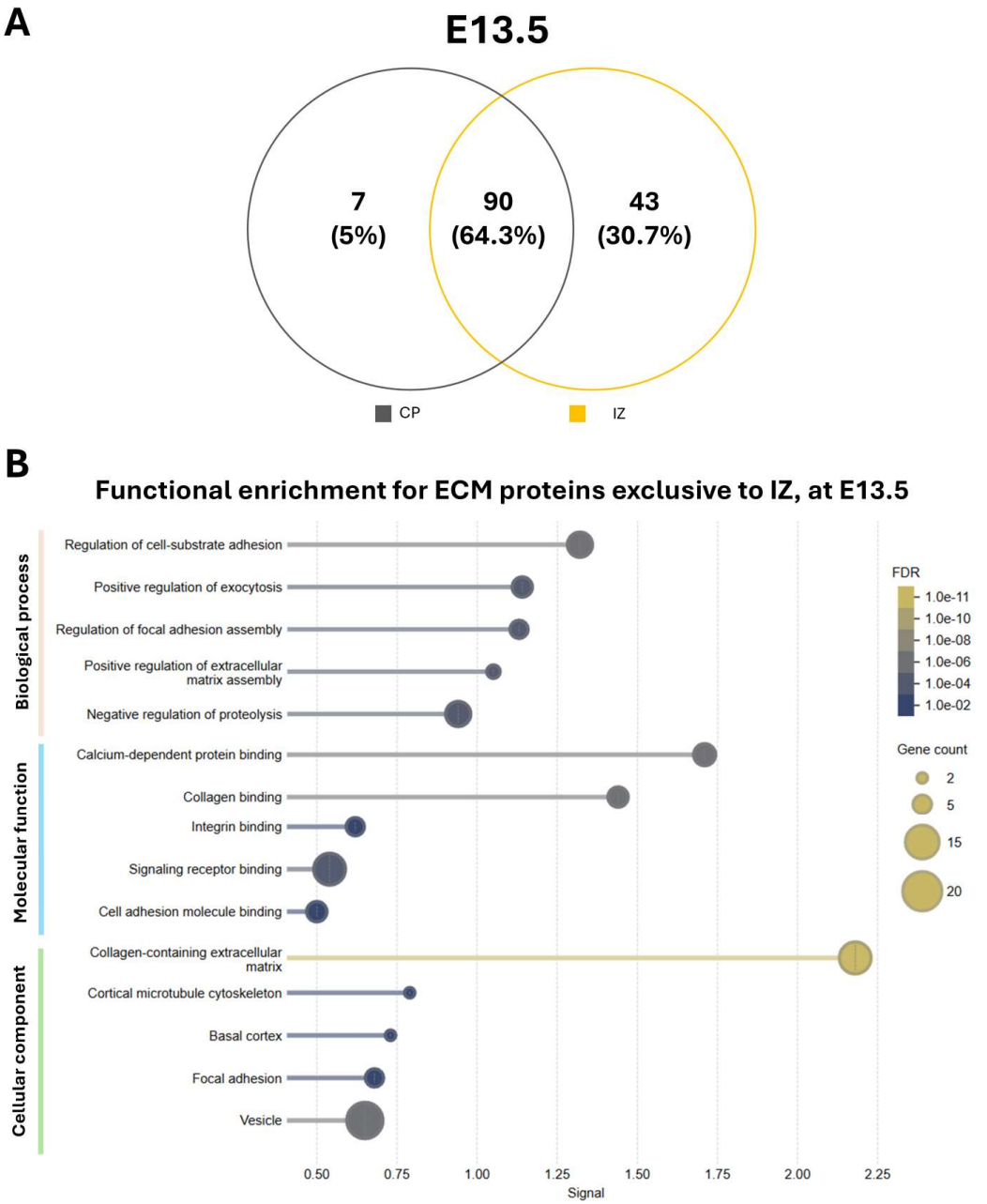

Figure 13: ***Violin plot and functional enrichment analyses.*** *Functional enrichment regroups proteins into GO-term lists that are sorted according to signal, gene count, and false discovery rate (FDR). The five most relevant GO-terms from three categories (i.e. biological process, molecular function, cellular component) are represented on the enrichment visualization, and sorted according to signal measures. Gene count indicates how many proteins from the network are annotated to the GO-term. FDR values are described using a color code, and indicate how significant the enrichment is.* ***A)*** *Violin plot comparing database of ECM-proteins detected in CP (grey) with database of ECM-proteins detected in SVZ/IZ (yellow) at E13.5.* ***B)*** *Functional enrichment for ECM proteins that were exclusively detected in SVZ/IZ at E13.5. N = 5 embryos, n = 5 CP samples per embryo, 5 SVZ/IZ samples per embryo*

Functional enrichment analyses of ECM-related proteins common to CP and SVZ/IZ reveals transversal processes to both zones. Results revealed similar terms than the ones common to E13.5 and E16.5, such as ***myelin sheath***, ***responses to IL-7***, ***calcium-dependent protein binding***, and others (***Fig. 12, Fig. 14***). Transversal processes to both zones are associated with GO-terms related to ***adhesion*** that were similar to those enriched in E13.5 SVZ/IZ.

Interestingly, ***cell projection, somatodendritic compartment***, and ***actin filament bundle assembly*** GO-terms are associated with exploratory behavior, where cINs are sensing the mechanical and chemical signals present in the microenvironment through actin-containing leading or branching processes.

Some GO-terms, such as ***smooth endoplasmic reticulum***, ***secretory vesicle*** and ***antioxidant activity***, are related to intracellular protein processing and secretory activity, which supports the hypothesis that cells are participating in the remodulation of ECM. On the other hand, cells are also responding to environmental signals that notably regulate their migration and survival, as indicated by ***response to wounding***, ***regulation of cell death***, and ***cellular response to IL-7*** GO-terms. ***Myelin sheath*** related proteins seem to be strongly present, in both regions but also at both stages, as indicated by the previous analyses (***Fig.14***).

Due to the small size of E13.5 CP-exclusive dataset, the network did not present significantly more interactions than expected, and no significant enrichment was detected. Among the 7 ECM-proteins detected, 2 actin proteins were present.

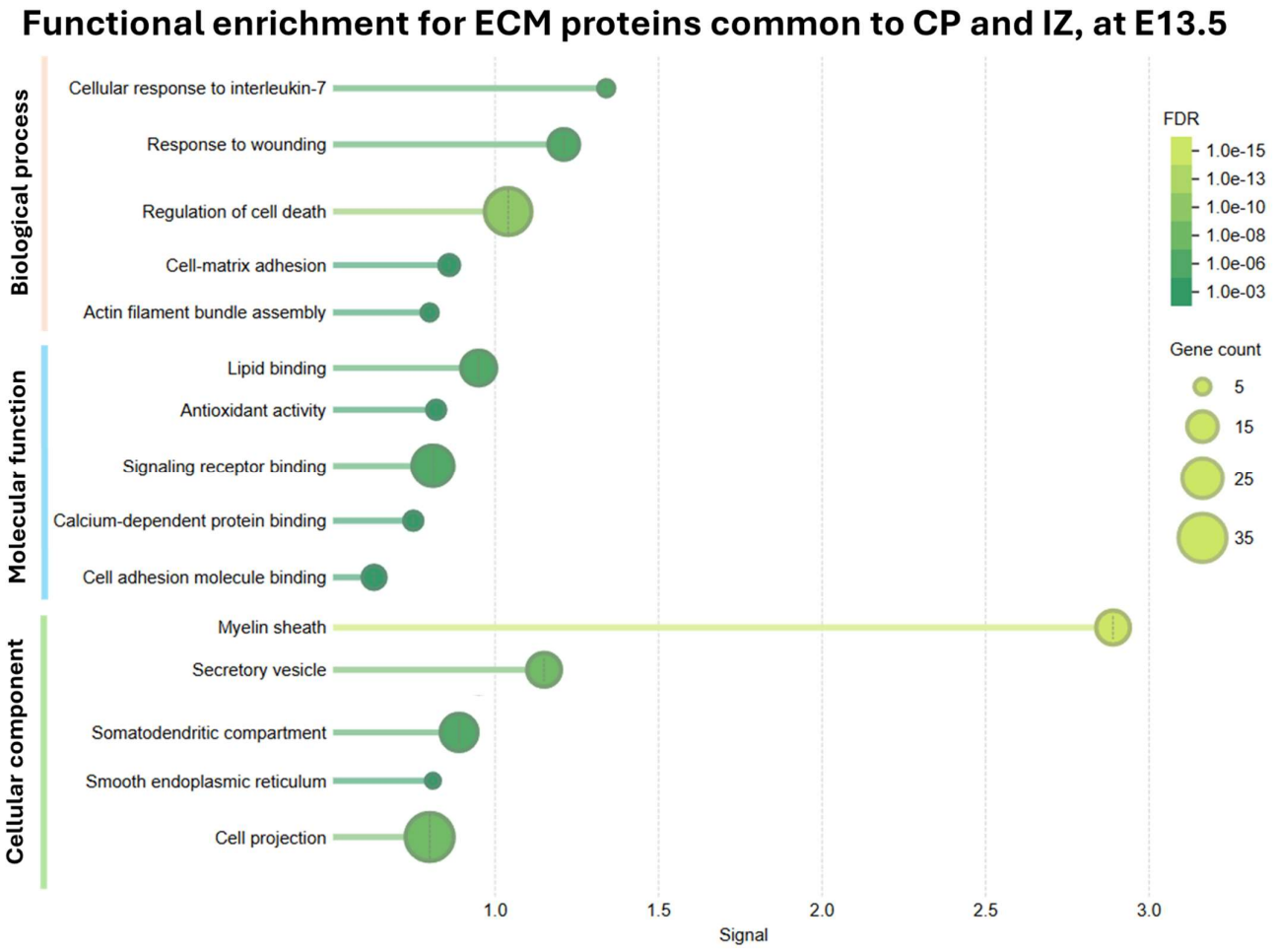

Figure 14: ***Visualization of functional enrichment analysis for ECM-related proteins common to CP and SVZ/IZ at E13.5.*** *Functional enrichment regroups proteins into GO-term lists that are sorted according to signal, gene count, and false discovery rate (FDR). The five most relevant GO-terms from three categories (i.e. biological process, molecular function, cellular component) are represented on the enrichment visualization, and sorted according to signal measures. Gene count indicates how many proteins from the network are annotated to the GO-term. FDR values are described using a color code, and indicate how significant the enrichment is. N = 5 embryos, 5 CP sample, 5 SVZ/IZ sample per embryo.*

At E16.5, more numerous neuronal cells are expected to be migrating in the CP, where they finally integrate in their appropriate cortical layer. Therefore, enrichment analyses were conducted on proteins exclusively detected in the CP, as well as proteins common to CP and SVZ/IZ.

Around 68% of proteins from E16.5 were exclusively present in CP. Approximately 30% of all E16.5 proteins were common to both regions, and less than 1% was exclusive to SVZ/IZZ (***Fig. 15A***).

Functional enrichment on E16.5 CP-exclusive dataset revealed GO-terms related to migration came out; ***positive regulation of cell migration***, ***substrate-dependent cell migration*** (***Fig. 15B***). Plus, proteins involved in cell growth and development appear enriched in the CP at E16.5, as indicated by GO-terms such as ***cell extension***, ***distal axon***, ***growth cone***, ***basal part of the cell***, ***regulation of cell size***, and ***regulation of anatomical structure morphogenesis***. Cell-ECM interactions and ECM remodelling processes are also taking place, as seen with GO-terms such as ***calcium-dependent protein binding***, ***actin filament binding***, ***signaling receptor binding***, ***regulation of proteolysis***, as well as those related to ***collagen*** and ***vesicles***.

The functional enrichment analyses on E16.5 ECM-related proteins (36 items, 1.3%) common to both CP and SVZ/IZ revealed that the highest enrichment is related to ***antioxidant activity*** GO-terms (***Fig. 16***). This reflects a high metabolic activity, correlated to the differentiation and complexification of neuronal cells in this zone. Plus, increased intracellular activity, especially protein processing, is also suggested by enriched GO-terms.

Interestingly, the enrichment of ***response to mechanical stimulus*** GO-term in this dataset indicates that cells migrating in CP at E16.5 are particularly sensitive to physical changes in the environment.

Due to the small size of E16.5 SVZ/IZ-exclusive dataset, the network did not present significantly more interactions than expected, and no significant enrichment was detected.

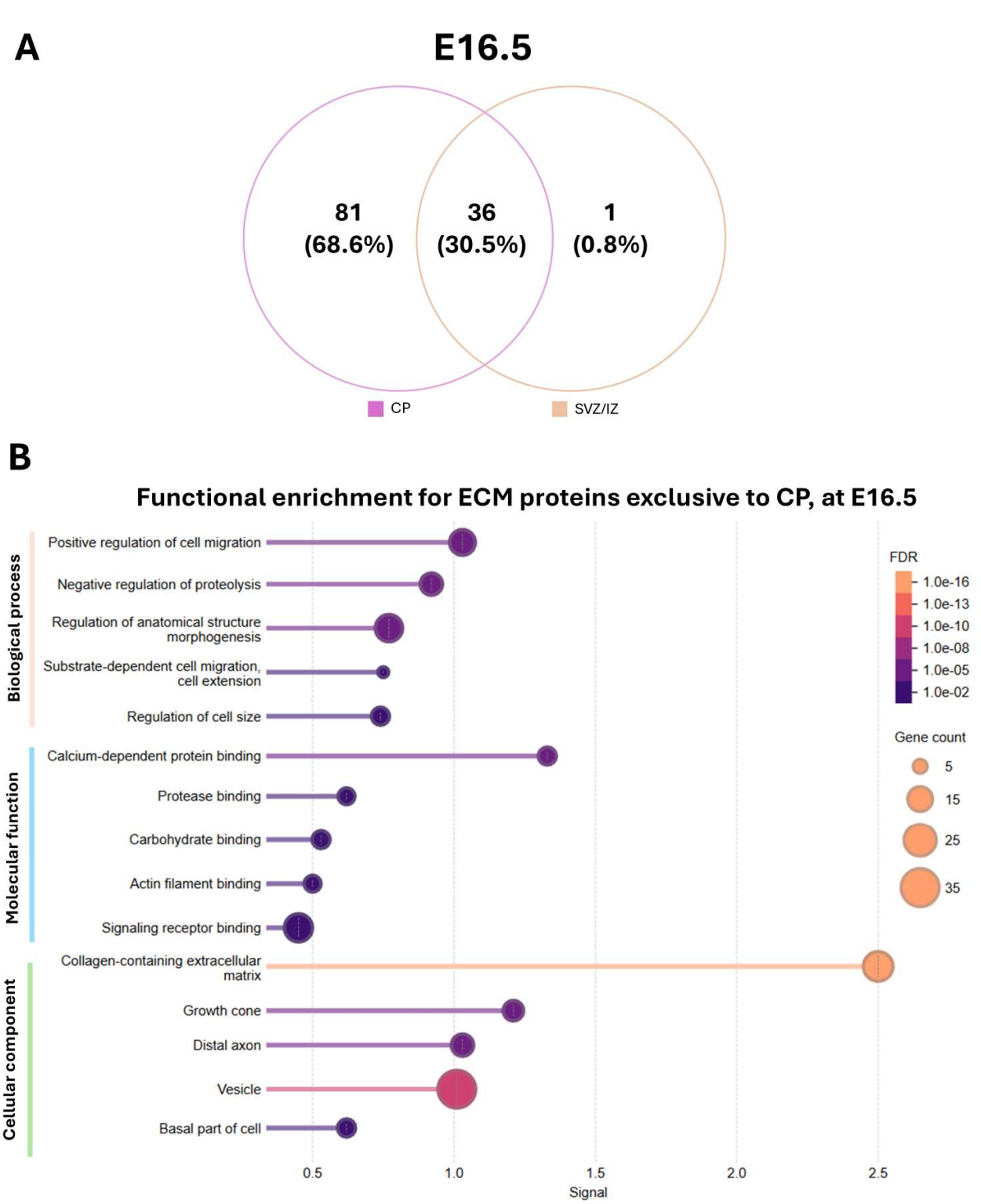

Figure 15: ***Visualization of functional enrichment analyses.*** *Functional enrichment regroups proteins into GO-term lists that are sorted according to signal, gene count, and false discovery rate (FDR). The five most relevant GO-terms from three categories (i.e. biological process, molecular function, cellular component) are represented on the enrichment visualization, and sorted according to signal measures. Gene count indicates how many proteins from the network are annotated to the GO-term. FDR values are described using a color code, and indicate how significant the enrichment is.* ***A)*** *Functional enrichment for ECM proteins that were exclusively detected in CP at E16.5.* ***B)*** *Functional enrichment for ECM proteins that were detected in CP and SVZ/IZ at E13.5. N = 1 embryo, n = 1 CP samples per embryo, 1 SVZ/IZ samples per embryo.*

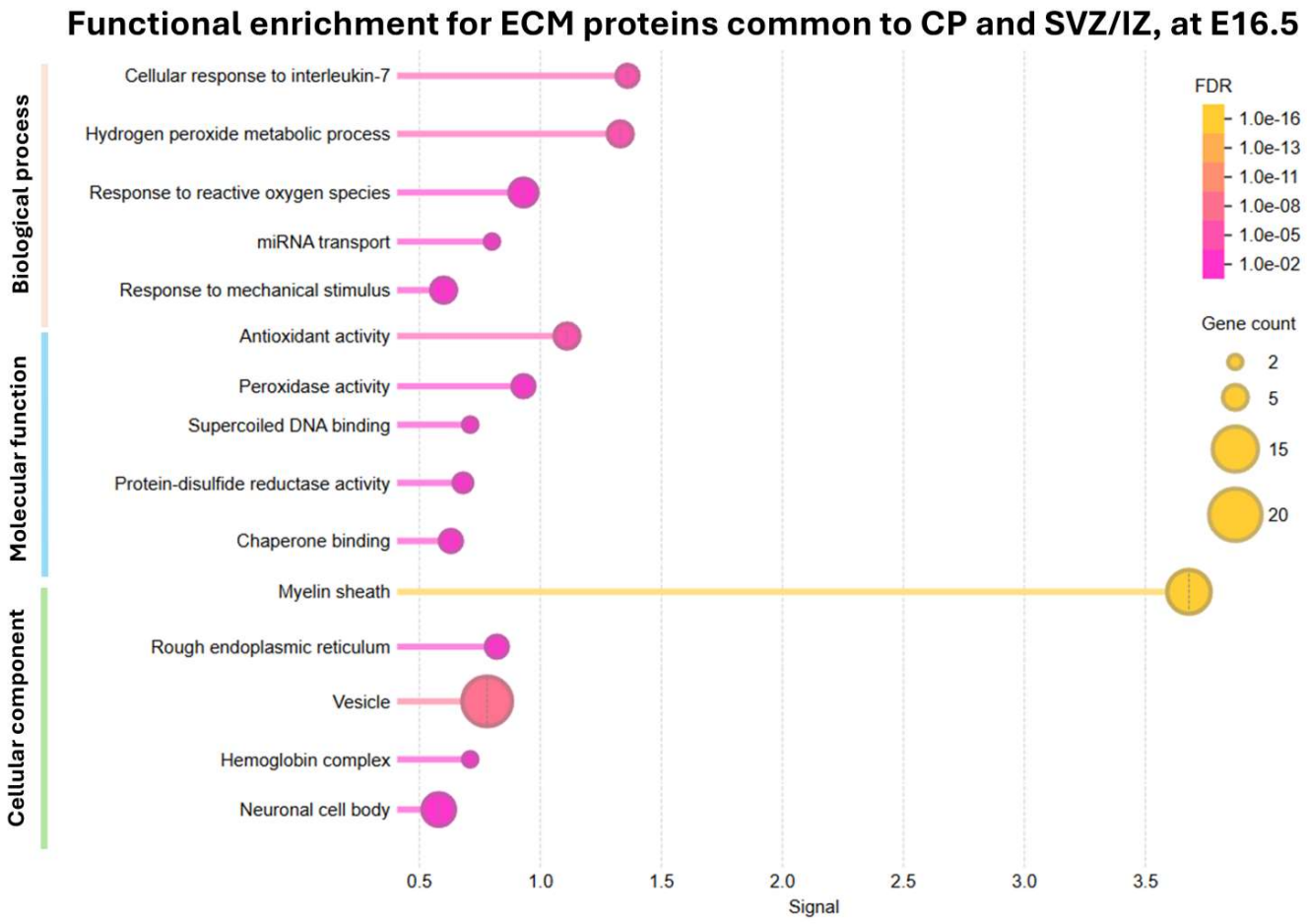

Figure 16: ***Visualization of functional enrichment analysis for ECM-related proteins common to CP and SVZ/IZ at E16.5.*** *Functional enrichment regroups proteins into GO-term lists that are sorted according to signal, gene count, and false discovery rate (FDR). The five most relevant GO-terms from three categories (i.e. biological process, molecular function, cellular component) are represented on the enrichment visualization, and sorted according to signal measures. Gene count indicates how many proteins from the network are annotated to the GO-term. FDR values are described using a color code, and indicate how significant the enrichment is. N = 1 embryo, 1 CP sample, 1 SVZ/IZ sample.*

Taken together, our results suggest a higher number of ECM-proteins at E13.5 compared to E16.5. While at E13.5, most of the ECM-proteins are common to both regions, most ECM-proteins are exclusive to CP at E16.5.

Although some GO-terms are often recurrent within functional enrichment analyses (*e.g.*, ***signaling receptor binding, cytoskeletal protein binding, collagen-containing ECM, cell adhesion molecule binding, calcium-dependent binding, integrin binding***), their enrichment in distinct stage- or zone-specific datasets indicates that these functions are carried out by different proteins, depending on the spatial and temporal context.

For instance, Dsp (protein involved in cell-cell adhesions), Vim (intermediate filament protein), and Lmnb1 (nuclear component of neuronal cells) were detected in both zones, at both stages. Actg1 (actin cytoskeleton protein), involved in responses to mechanical cues, is enriched at E16.5 but not at E13.5. Interestingly, Shtn1 (Shootin1b clutch) was exclusively detected in CP region at E16.5 (***Table 2***). These differentially expressed proteins show that subgroups of proteins are specific to cortical zones and/or developmental stages.

		E13.5		E16.5	
Gene Product	**Role**	**IZ**	**CP**	**SVZ/IZ**	**CP**
Has1	Hyaluronan Synthase	+	-	-	-
Ncan	ECM proteoglycan	-	-	-	+
Ncam1	Neural cell adhesion molecule	+	-	-	+
Colgalt1	ECM protein	+	-	-	-
Efnb1	cIN migration	+	-	-	+
Dpysl3		+	+	-	-
Mdk		+	+	-	-
Smad3		+	-	-	-
Cd81		+	-	-	-
Ctnb1		-	-	+	+
Shtn1		-	-	-	+
Cdh13		-	-	-	+
Dsp	Cell-cell adhesion	+	+	+	+
Vim	Intermediate filament	+	+	+	+
Lmnb1	Nuclear membrane	+	+	+	+
Rhoa	Cytoskeleton organization	+	+	-	-
Myh10		+	+	-	-
Src	Focal adhesions	+	-	-	-
Itgb1		+	-	-	-
Arhgdia	Response to mechanical stimulus	+	+	+	+
Actg1		-	-	+	+

***Table 2*: Table of protein-specific enrichments in each ECM-related proteins subset.**

DISCUSSION

5. DISCUSSION

5.1. YAP/TAZ pathway is involved in modulation of cortical interneuron migration

During development, YAP/TAZ pathway acts as a master regulator of cell proliferation, differentiation and survival. Dephosphorylation of these transcription coactivators, which can be triggered under high mechanical tension, promotes their nuclear translocation, where they regulate gene expression.

Interestingly, a recent study showed that the peptide TAT-PDHPS1 inhibits Yap1, by increasing the levels of p-Yap1. Similarly, we also found both accumulation of pYap1 and decrease of total-Yap1 in cortical neurons (***Fig. 5***). In addition, our results indicate for the first time that TAT-PDHPS1 inhibitor also increases the levels of p-Taz, implying that TAT-PDHPS2 peptide is not a specific YAP inhibitor.

Despite the involvement of Yap1 in the proliferation of neural progenitor cells, little is known about its role in migrating neurons. Our results show impairment of E13.5 cIN migration upon treatment with TAT-PDHPS1, suggesting that Yap/Taz pathway regulates the migration of cINs during development (***Fig. 6, 7***). However, TAT-PDHPS1 treatment might affect the activity of many other proteins, since the peptide binds to upstream phosphatases PTPA and PP2A. Hence, further investigation are required to clarify the respective roles of Yap1 and Taz in cIN migration. Particularly, Yap1 knockdown by RNA interference would rule out unspecific effects of TAT-PDHPS1 through PTPA/PP2A downstream effectors. Plus, this inhibition strategy would not affect Taz activity, allowing a more precise understanding of Yap1 function. Additionally, this approach would enable the study of Yap1 role specifically in cINs, without impacting neurons from the cortical feeder.

Eventually, future investigations will be necessary to determine the molecular mechanisms by which Yap1 regulates migration of cIN. Although our findings support a role of Yap1 in promoting cIN migration at E13.5, the downstream molecular effectors involved remain unknown. In cancer studies, it has been shown that TAT-PDHPS1 treatment significantly downregulates the expression of Yap1 target genes, such as CYR61 and CTGF.[69] These genes

are involved in cellular processes including adhesion, migration, and response to extracellular cues. However, their contribution in cIN migration during neocortical development remains unexplored. Lastly, although compelling evidences suggest that Yap1 activity is promoted in response to mechanical forces, we are not able yet to determine if cIN migration defects after Yap1 inhibition is mediated by disruption of mechanotransduction signaling. To gain insight on the mechanical regulation of Yap1 activity in cINs, an experimental strategy could involve cINs culture on substrates with increasing stiffness, and to monitor the localization of Yap1 in the nucleus.

The understanding of how YAP/TAZ regulate cIN migration could provide important insights into neurodevelopmental pathologies. Indeed, defective cIN migration is often implicated in neurological disorders, such as epilepsy and cortical malformations. Recent studies have shown that dysregulation of YAP can contribute to heterotopia and megalencephaly, which are frequently associated with epileptic phenotype. Moreover, YAP has been identified as a downstream effector of mechanosensitive channels, such as TRPV4, involved in epileptic seizures Together, these findings suggest that YAP/TAZ not only respond to mechanical properties of the developing brain, but may also represent a critical candidate for brain and excitability disorders. Investigating YAP/TAZ role in cIN migration could offer new perspectives on such neurodevelopmental conditions.[61, 66]

5.2. Embryonic cortical interneurons interact mechanically with their environment

Interactions between cells and ECM are bidirectional: while the ECM provides mechanical signals to the surrounding cells, migrating neurons also exert forces on their substrate in order to sense the environment and to migrate. Here, we demonstrate that E13.5 cINs display traction forces on a PAA hydrogel (***Fig. 8***).

Our results revealed that E13.5 cINs generate traction forces averaging around 10 Pa. (***Fig. 9***) Consistent with other studies [36,48-50], the axonal growth cone emerged as the main site of traction forces generation. This structure is essential for environment sensing and generation of pulling forces through actin and microtubule cytoskeleton. Notably, the cIN analyzed at T0

exhibited a branched morphology, suggestive of active exploration and correlating with the higher magnitude of traction forces recorded at this timepoint (***Fig. 9***).

The reduction of force intensity between two timepoints indicates that forces exerted by cINs are transient and dynamic, rather than constant. This reflects with alternating phases of nucleokinesis and pausing, and is in line with cytoskeleton remodelling events required for cIN migration.

While the highest forces were detected at the growth cone, localized forces near the nucleus were also observed. These may be attributed to contractions of the actomyosin cytoskeleton, which transmits force to the nucleus through structures such as the LINC complex during nuclear translocation.[57]

These preliminary results support the hypothesis that cINs are dynamically interacting with the ECM through generation of intrinsic traction forces, required for proper migration. However, due to the low number of cells analyzed, further experiments are required to evaluate more accurately the characteristics of forces generated. Moreover, investigations of the potential involvement of mechanotransduction pathways, including the role of YAP/TAZ, in regulating these traction forces would allow to highlight further mechanisms of cIN migration.

In addition, recent work indicate a correlation between nuclear Yap and the magnitude of traction forces. [72,73] Together with the effect of Yap1 observed in the migration of cINs (***Fig. 6, 7***), this points to Yap1 as molecular candidate in the generation of traction forces. In this line, our preliminary proteomics results detected Shootin1 in the CP of E16.5 cINs. Of interest, the role of Shootin1a in the production of traction forces during axonal growth in hippocampal neurons has been reported.[74,75] Recent evidences indicates that Shootin1b would also engage a mechanical clutch to produce traction forces required for the migration of olfactory interneurons.[48] Further investigations on Shootin1 protein are further required to potentially highlight a key mechanotransducer in cIN migration.

5.3. Differential expression of ECM-related proteins between developmental stages and between neocortical zones

Communication between cells and the ECM is crucial for numerous biological processes, including cINs migration, which relies on both chemical and mechanical extracellular cues. Previous data from our laboratory have highlighted differences of cIN migratory behaviors between the SVZ/IZ and the CP, as well as through development. Therefore, the ECM composition emerges as a potential contributor to this observation.

Consistent with existing literature, our mass spectrometry-based analysis revealed that at both E13.5 and E16.5, the ECM contains proteins associated with adhesion structures such as focal adhesions, integrin-binding molecules, and cell adhesion components.[37, 43, 45, 76] These are essential for mediating interactions, such as mechanotransduction, between cells and their substrate and are well-known effectors of mechanotransduction. Notably, while these functional categories were recurrent across all zones and stages, the specific proteins associated with them differed. This suggests that although the biological processes involved in cIN migration are preserved, their molecular execution is finely tuned in a stage- and region-specific manner.

While these functional categories were recurrent across all zones and stages, the specific proteins associated with them differed. This suggests that although the biological processes involved are preserved, their molecular effectors are differentially expressed in regions, and during developmental stages. Future research focusing on candidate proteins could highlight specific processes, such as YAP/TAZ, vinculin, or shootin1 which have been already show to contribute to mechanotransduction [77].

Even though few GO-terms were associated with a cellular response to chemical signals, the consistent enrichment of calcium-dependent binding proteins and cytoskeletal binding proteins across all datasets suggests that migrating cells are also sensitive to mechanical stimuli [52]. Moreover, binding processes to cytoskeletal components at both stages show that cells are actively responding to mechanical cues by cytoskeleton remodeling, which is crucial for motility and force transmission.

In addition, our analyses identified distinct molecular signatures associated with the CP and SVZ/IZ. At E13.5, the IZ showed a strong enrichment in terms associated with ECM remodelling. The constitutive enrichment for protein synthesis and exocytosis processes suggests that the ECM is actively remodeled and that migrating cells might be contributing by secreting new components.
At E16.5, the CP exhibited GO-terms reflecting a stage where neurons reach their final positioning and begin to maturate. Furthermore, the proteins shared between CP and SVZ/IZ at E16.5 showed a unique signature of oxidative stress response, suggesting that cells in both zones are undergoing intense intracellular processing, likely linked with cell differentiation, metabolic demands and synaptic development.

Although our experimental approach does not allow us to directly attribute these proteins to cINs mechanisms given the cellular heterogeneity within the dissected cortical regions, both dissected zones are known to be enriched in migrating cINs. Plus, the recurrent enrichment of GO-terms related to ***axonal growth cone*** and ***filopodia*** strongly suggests that migration processes are active in these zones. Indeed, these structures are known to be essential for exploration, directionality, and movement forces during tangential migration, particularly for cINs. Therefore, even though these preliminary data do not provide cell-type specificity, they are consistent with tangential migration processes and an integration of external mechanical cues.

Both microdissected CP and SVZ/IZ zones are enriched in cINs. Therefore, proteins identified at all stages and in all zones, such as Dsp, Lmnb1 or Vim, could be major actors in cINs, and further investigations of recurrent proteins may highlight key proteins for cIN migration. Additionnally, differentially expressed proteins, such as Shtn1 or other proteins related to mechanotransduction (such as Actg1) could underlie key mechanisms responsible for different migratory behavior of cIN across development.

It is important to note that a contamination by solvents was detected in all our samples, maybe responsible for the limited number of E16.5 samples. Therefore, these results should be considered as preliminary data only. Further investigations will required more accurate strategies to specifically explore ECM-cIN interactions. One promising direction would be to

analyze acellular brain slices, allowing the isolation of ECM components in the absence of cellular content. Additionally, intersecting our proteomic data with literature databases could help to isolate ECM-related proteins only, and to exclude intracellular proteins. Such strategies would enable a better understanding of the ECM proteome in which cINs migrate during development.

Nevertheless, our preliminary findings reveal that while certain core mechanisms – such as ***ECM binding***, ***cytoskeletal engagement***, and ***signal perception*** – are conserved throughout development, they are achieved via distinct molecular players depending on both the spatial and temporal context. These differences reflect the evolution of the microenvironment where cIN are migrating, and suggest that ECM remodelling through development represents a potential candidate for cINs changes in migratory behavior.

5.4. Conclusions and perspectives

In this master's thesis, we explored the contribution of mechanical forces to the regulation of cIN tangential migration during brain development, based on emerging evidence implicating mechanotransduction in this process. First, we demonstrated that the role of the mechanosensors YAP/TAZ in the regulation of cIN migration. Secondly, we revealed that cINs exert localized, dynamic traction forces, particularly around the growth cone and nucleus, suggesting that intrinsic mechanical force generation is associated to environmental sensing and nucleokinesis. Given these interactions between the migrating cIN and its environment, we showed that while ECM-related functions are mainly preserved across developmental stages and cortical regions (CP and SVZ/IZ), they are carried out by distinct protein actors, and we identified protein candidates that might explain different migratory behaviors of cINs.

Together, these findings highlight that tangentially migrating cINs are not only subjected to external mechanical cues, but also generate active traction forces. This work strengthens the notion that mechanical signaling is essential for cIN migration, and opens new perspectives for investigating the interactions between migrating neurons and brain ECM and mediated by mechanotransduction. A deeper understanding of these mechanisms may offer novel insights into the pathophysiology of neurodevelopmental disorders such as cortical malformations and epilepsy, in which altered cIN migration is a key mechanism.

BIBLIOGRAPHY

6. BIBLIOGRAPHY

1. Chen VS, Morrison JP, Southwell MF, Foley JF, Bolon B, Elmore SA. Histology atlas of the developing prenatal and postnatal mouse central nervous system, with emphasis on prenatal days E7.5 to E18.5. *Toxicol Pathol*. 2017; 45(6): 705-744

2. Bolon B, Ward JM. Anatomy and physiology of the developing mouse and placenta. In: Kaufman MH, Bard JBL, editors. *Pathology of the developing mouse*. 1st ed. Boca Raton (FL):CRC Press; 2015. p. 39-98

3. Agirman G, Broix L, Nguyen L. Cerebral cortex development: an outside-in perspective. *FEBS Letters*. 2017; 591: 3978-3992

4. Corbin JG, Nery S, Fishell G. Telencephalic cells take a tangent: non-radial migration in the mammalian forebrain. *Nature neuroscience*. 2001; 4: 1177-1182

5. Appan D, Hsu SM, Hsu WN, Chou SJ. Patterning the cerebral cortex into distinct functional domains during development. *Current Opinion in Neurobiology*. 2023; 80: 102689

6. Angevine J, Sideman R. Autoradiographic study of cell migration during histogenesis of cerebral cortex in the mouse. *Nature*. 1961; 192: 766–768

7. Ang J ESBC, Haydar TF, Gluncic V, Rakic P. Four-dimensional migratory coordinates of GABAergic interneurons in the developing mouse cortex. *The Journal of Neuroscience*. 2003; 23(13): 5805-5815

8. Kriegstein AR, Noctor SC. Patterns of neuronal migration in the embryonic cortex. *TRENDS in Neurosciences*. 2004; 27(7): 392-399

9. Anderson SA, Kaznowski CE, Horn C, Rubenstein JLR, McConnel SK. Distinct origins of neocortical projection neurons and interneurons in vivo. *Ceberal Cortex*. 2002; 12: 702-709

10. Fazzari P, Mortimer N, Yabut O, Vogt D, Pla R. Cortical distribution of GABAergic interneurons is determined by migration time and brain size. *Development*. 2020; 147(14): dev18503

11. Southwell DG, Paredes MF, Galvao RP, Jones DL, Froemke RC, Sebe JY, *et al*. Intrinsically determined cell death of developing cortical interneurons. *Nature.* 2012; 491: 109-11

12. Batista-Brito R, Ward C, Fishell G. The generation of cortical interneuron. In: Rubenstein JL, Rakic P, editors. *Patterning and cell type specification in the developing CNS and PNS* (2nd ed). San Diego: Academic Press; 2020. p. 461-478

13. Lodato S, Arlotta P. Generating neuronal diversity in the mammalian cerebral cortex. *Annu Rev Cell Dev Biol*. 2015; 31: 699-72

14. Greig LC, Woodworth MB, Galazo MJ, Padmanabhan H, Macklis JD. Molecular logical of neocortical projection neuron specification, development, and diversity. *Nature Reviews Neuroscience*. 2017; 14: 755-769

15. Wonders CP, Anderson SA. The origin and specification of cortical interneurons. *Nature Reviews Neuroscience*. 2006: 7; 687-696

16. Koh W, Kwak H, Cheong E, Lee J. GABA tone regulation and its cognitive functions in the brain. *Nat Rev Neurosci.* 2023; 24(9): 523-539

17. Bellion A, Baudoin JP, Alvarez C, Bornens M, Métin C. Nucleokinesis in tangentially migrating neurons comprises two alternating phases: Forward migration of the Golgi/centrosome associated with centrosome splitting and myosin contraction at the rear. *J Neurosci*. 2005;25(24):5691-5699

18. Tremblay R, Lee S, Rudy B. GABAergic interneurons in the neocortex: from cellular properties to circuits. *Neuron*. 2016;91:260-292

19. Lim L, Mi D, Llorca A, Marín O. Development and functional diversification of cortical interneurons. *Neuron*. 2018:100;294-313

20. Allen NJ, Lyons DA. Glia as architects of central nervous system formation and function. *Science*. 2018; 362(6411):181-185

21. Reemst K, Noctor SC, Lucassen PJ, Hol EM. The indispensable roles of microglia and astrocytes during brain development. *Front. Jum. Neurosci*. 2016; 10: 566

22. Tanaka DH, Maekawa K, Yanagawa Y, Obata K, Murakami F. Multidirectional and multizonal tangential migration of GABAergic interneurons in the developing cerebral cortex. *Development*. 2006; 133: 2167-2176

23. Lim L, Pakan JMP, Selten MM, Marques-Smith A, Llorca A, Bae SE, *et al*. Optimization of interneuron function by direct coupling of cell migration and axonal targeting. *Nature Neuroscience*. 2018; 21: 920-931

24. Toudji I, Toumi A, Chamberland E, Rossignol E. Interneuron odyssey : molecular mechanisms of tangential migration. *Frontiers in Neural Circuits*. 2023;17:1256455

25. Tamamaki N, Fujimori K, Nojyo Y, Kaneko T, Takauji R. Evidence that Sema3A and Sema3F regulate the migration of GABAergic neurons in the developing neocortex. *J Comp Neurol*. 2003; 455(2): 238-248

26. Marín O, Yaron A, Bagri A, Tessier-Lavigne M, Rubenstein JL. Sorting of striatal and cortical interneuron regulated by semaphorin-neuropilin interactions. *Science*. 2001; 293(5531): 872-875

27. Rudolph J, Zimmer G, teinecke A, Barchmann S, Bolz J. Ephrins guide migrating cortical interneurons in the basal telecenphalon. *Cell Adhesion & Migration*. 2010; 4(3): 400-408

28. Ogawa M, Miyata T, Nakajimat K, Yagyu K, Seike M, Ikenaka K, *et al*. The reeler gene-associated antigen on cajal-retzius neurons is a crucial molecule for laminar organization of cortical interneurons. *Neuron*. 1995; 14(5): 899-912

29. Marín O, Rubenstein JLR. A long, remarkable journey : tangential migration in the telencephalon. *Nature*. 2001; 2: 780-790

30. Fazzari P, Paternain AV, Valiente M, Pla Ramón, Luján R, Lloyd K, *et al*. Control of cortical GABA circuitry development by Nrg1 and ErbB4 signalling. *Nature*. 2010; 464: 1376-1382

31. Tiveron MC, Rossel M, Moepps B, Zhang YL, Seidenfaden R, Favor J, *et al*. Molecular interaction between projection neuron precursor and invading interneurons via stromal-derived factor 1 (CXCL12)/CXCR4 signaling in the cortical subventricular zone/intermediate zone. *The Journal of Neuroscience*. 2006; 26(51): 13276-13278

32. Borrell V, Marín O. Meninges control tangential migration of hem-derived Cajal-Retzius cells via CXCL12/CXCR4 signaling. *Nature Neuroscience*. 2006; 9: 1284-1293

33. López-Bendito G, Sánchez-Alcañiz JA, Pola R, Borrel V, Picó E, Valdeolmillos M, *et al*. Chemokine signaling conrols intracortical migration and final distribution of GABAergic interneurons. *J Neurosci*. 2008; 28(7): 1613-1624

34. Wang DD, Kriegstein AR. Defining the role of GABA in cortical development. *J Physiol*. 2009; 587.9; 1873-1879

35. Caviness VSJ. Neocortical histogenesis in normal and reeler mice: a developmental study based upon [^{3}H]-thymidine autoradiography. *Developmental Brain Research*. 1982;4:293-302

36. Franze K, Janmey PA, Guck J. Mechanics in neuronal development and repair. *Annu. Rev. Biomed. Eng*. 2013; 15: 277-251

37. Franco SJ, Müller U. ECM functions during neuronal migration and lamination in the mammalian central nervous system. *Dev Neurobiol*. 2011; 71(11): 889-900

38. Leclech C, Renner M, Villard C, Métin C. Topographical cues control the morphology and dynamics of migrating cortical interneurons. *Biomaterials*. 2019; 214: 119194

39. Jaalouk DE, Lammerding J. Mechanotransduction gone ewry. *Nature Reviews*. 2009; 10: 63-73

40. Pillai EK. Franze K. Mechanics in the nervous system: from development to disease. *Neuron*. 2024; 112: 342-361

41. Iwashita M, Kataoka N, Toida K, Kosodo Y. Systematic profiling of spatiotemporal tissue and cellular stiffness in the developing brain. *Development*. 2014; 141: 2793-3798

42. Nagasaka A, Miyata T. Comparison of the mechanical properties between the convex and concave inner/apical surfaces of the developing cerebrum. *Frontiers in Cell and Developmental Biology*. 2021; 9:702068

43. Long KR, Huttner WB. How the extracellular matrix shapes neural development. *Open Biol*.2018; 9: 180216

44. Javier-Torrent M, Zimmer-Bensh G, Nguyen L. Mechanical forces orchestrate brain development. *Trends in Neurosciences*. 2021; 44(2): 110-121

45. Amin S, Borrell V. The extracellular matrix in the evolution of cortical development and folding *Front. Cell Dev. Biol*. 8:604448

46. Lilja J, Ivaska J. Integrin activity in neuronal connectivity. *Journal of Cell Science*. 2018; 131: jcs212803

47. Martino F, Perestrelo AR, Vinarský V, Pagliari S, Forte G. Cellular mechanotransduction : from tension to function. *Front. Physiol*. 2018; 9: 824

48. Minegishi T, Inagaki N. Forces to drive neuronal migration steps. *Front. Cell Dev. Biol.* 8:863

49. Betz T, Koch D, Lu YB, Franze K, Käs JA. Growth cones as soft and weak force generators. *PNAS*. 2011; 108(33): 13420-13425

50. Nakajima C, Sawada M, Umeda E, Takagi Y, Nakashima N, Kuboyama K, *et al*. Identification of the growth cone as a probe and driver of neuronal migration in the injured brain. *Nature Communications*. 2024; 15: 1877

51. Toriyama M, Kozawa S, Sakumara Y, Inagaki N. Conversion of a signal into forces for axon outgrowth through Pak1-mediated Shootin1 phosphorylation. *Current Biology*. 2013; 23: 529-534

52. Jin P, Jan LY, Jan YN. Mechanosensitive ion channels: structural features relevant to mechanotransduction mechanisms. *Annu. Rev. Neurosci*. 2020; 43: 207-229

53. Sun Z, Guo S, Fässler R. Integrin-mediated mechanotransduction. *J. Cell Biol*. 2016; 215(4): 445-456

54. Wang N. Review of cellular mechanotransfuction. *J Phys D Appl Phys*. 2017; 50(23)

55. Bachman M, Kukkurainen S, Hytönen VP, Wehrle-Haller B. Cell adhesion by integrins. *Physiol Rev*. 2019; 99: 1655-1699

56. Seong J, Wang N, Wang Y. Mechanotransduction at focal adhesions: from physiology to cancer development. *J Cell Mol Med*. 2013; 17(5): 597-604

57. Khilan AA, Al-Maslamani NA, Horn HF. Cell stretchers and the LINC complex in mechanotransduction. *Archives of Biochemistry and Biophysics*. 2021;702:108829

58. Echarri A. A multisensory network drives nuclear mechanoadaptation. *Biomolecules*. 2022; 12: 404

59. Zhao B, Li L, Tumaneng K, Wang CY, Guan KL. A coordinated phosphorylation by Lats and CK1 regulates YAP stability through $SCF^{\beta-TRC}$. *Genes & Development*. 2010; 24: 72-85

60. Sun Y, Yong KMA, Villa-Diaz LG, Zhang X, Chen W, Philson R, *et al*. Hippo/YAP-mediated rigidity-dependent motor neuron differentiation of human pluripotent stem cells. *Nature Materials*. 2014; 13: 599-604

61. Liu WA, Chen S, Li Z, Lee CH, Mirzaa G, Bobyns WB, *et al*. PRD3 dysfunction in conjunction ith dynamic HIPPO signaling drives cortical enlargement with massive heterotopia. *Genes & Development*.2018; 32: 763-780

62. Elosegui-Artola A, Andreu I, Beedle AEM, Lezamiz A, Uroz M, Kosmalska AJ, *et al*. Force triggers YAP nuclear entry by regulating transport across nuclear pores. *Cell*. 2017; 171: 1397-1410

63. Hadden WJ, Young JL, Holle AW, McFetridge ML, Kim DY, Wijesinghe P, Taylor-Weiner H, *et al*. Stem cell migration and mechanotransduction on linear stiffness gradient hydrogels. *PNAS*. 2017; 114(22): 5647-5652

64. Dupont S. Role of YAP/TAZ in cell-matrix adhesion-mediated signalling and mechanotransduction. *Experimental Cell Research*. 2016; 343: 42-53

65. Piccolo S, Dupont S, Cordenonsi M. The biology of YAP/TAZ: Hippo signling and beyond. *Physiol Rev*. 2014; 94: 1287-1312

66. Zheng Q, Liu H, Yu W, Dong Y, Zhou L, Deng W, *et al*. Mechanical properties of the brain: focus on the essential role of Piezo1-mediated mechanotransduction in the CNS. *Brain Behav*. 2023; 13: e3136

67. Pathak MM, Nourse JL, Tran T, Tombola F. Stretch-activated ion channel Piezo1 directs lineage choice in human neural stem cells. *PNAS*. 2014; 111(45): 16148-16153

68. Lepiemme F, Stoufflet J, Javier-Torrent M, Mazzucchelli G, Silva C.G, Nguyen L. Oligodendrocyte precursors guide interneuron migration by unidirectional contact repulsion. *Science;* 2022; 376(6595): eabn6204

69. Pan X, Geng Z, Li J, Li X, Zhang M, Wang X, *et al*. Peptide PDHPS1 inhibits ovarian cancer growth through disrupting YAP signaling. *Mol Cancer Ther*. 2022; 21: 1160-1170

70. Nardone G, Oliver-De La Crux J, Vrbsky J, Martini C, Pribyl J, Skladal P, *et al*. YAP regulates cell mechanics by controlling focal adhesion assembly. *Nature communications*. 2017; 8: 15321.

71. Allen NJ, Lyons DA. Glia as architects of central nervous system formation and function. *Science*. 2018; 362(6411): 181–185

72. Zhao, B. *et al*. Inactivation of YAP oncoprotein by the Hippo pathway is involved in cell contact inhibition and tissue growth control. *Gene Dev*. 2007; 21: 2747–2761

73. Aragona, M. et al. A mechanical checkpoint controls multicellular growth through YAP/TAZ regulation by actin-processing factors. *Cell*. 2013; 154: 1047–1059

74. Shimada T, Toriyama M, Uemura K, Kamiguchi H, Sugiura T, Watanabe N, et al. Shootin1 interacts with actin retrograde flow and L1-CAM to promote axon outgrowth. *J Cell Biol*. 2008; 181(5): 817–829

75. Kubo Y, Baba K, Toriyama M, Minegishi T, Sugiura T, Kozawa S, *et al*. Shootin1–cortactin interaction mediates signal–force transduction for axon outgrowth. *J Cell Biol*. 2015; 210(4): 663–676

76. Robles E, Gómez TM. Focal adhesion kinase signaling at sites of integrin-mediated adhesion controls axon pathfinding. *Nat Neurosci*. 2006; 11: 1274–1283

77. Wang DY, Melero C, Albaraky A, Atherton P, Janser KA, Dimitracopoulos A. Vinculin is required for neuronal mechanosensing but not for axon outgrowth. *Experimental Cell Research*. 2021; 112805

SUPPLEMENTARY FIGURES

7. SUPPLEMENTARY FIGURES

Solution	Composition
8% separation gel	8% Acrylamide, 375 mM Tris, 0.1% SDS, 0.1% APS, 0.01% TEMED
5% stacking gel	5% Acrylamide, 125 mM Tris, 0.1% SDS, 0.1% APS, 0.01% TEMED
Running buffer (pH 8.3)	0.2 M Glycine, 20 mM *Tris-pufferan,* 3.47 mM SDS in H_2O
Transfer buffer (pH 8.3)	0.2 M Glycine, 20 mM *Tris-pufferan*, 20% Methanol in H_2O
Stripping buffer (pH 2.2)	0.2 M Glycine, 3.47 mM SDS, 1% *Tween-20* in H_2O
TBS 10X (pH 7.5)	0.5 M Tris, 1.5 M NaCl in H_2O
TBS-T	0.5 M Tris, 1.5 M NaCl, 0.1% *Tween-20* in H_2O
RIPA buffer	50 mM Tris-HCl, 150 mM NaCl, 1 mM EDTA, 1% Triton, 1% Na-deoxycholate, 0.1% SDS
Blocking solution	5% bovine serum albumin (BSA) in TBS-T

***Supplementary Table 1*: Composition of solutions used for Western blotting.**

GO-term list name	GO-term list accession
Extracellular matrix	GO:0031012
Extracellular space	GO:0005615
Regulation of extracellular matrix disassembly	GO:0010715
Regulation of extracellular matrix assembly	GO:1901201
Extracellular regulation of signal transduction	GO:1900115
Substrate-dependent cell migration, cell extension	GO:0006930
Cell-matrix adhesion	GO:0007160

***Supplementary Table 2*: Recapitulative table of GO-terms lists names and accessions included in the ECM proteins reference database.**

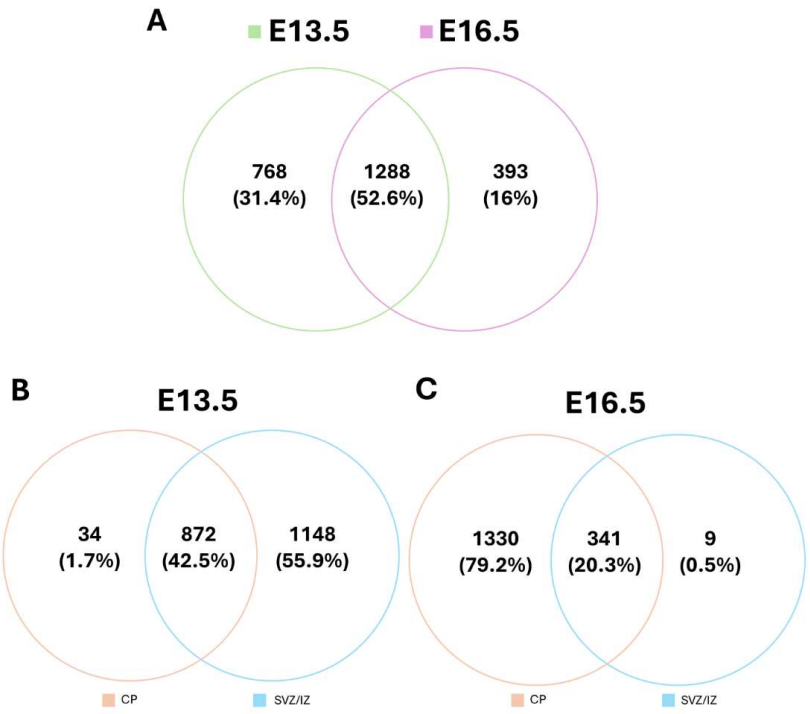

Supplementary Figure 1*: Amounts of all identified proteins subdivided into different datasets. All identified proteins include intracellular and ECM proteins.** ***A) *Violin plot comparing database of all proteins detected at E13.5 (green) with database of all proteins detected at E16.5 (purple), both in CP and in SVZ/IZ samples.* ***B)*** *Violin plot comparing dataset of proteins exclusively identified in CP (orange) with dataset of proteins exclusively identified in SVZ/IZ (blue), at E13.5. N = 5 embryos, n = 5 CP samples, 5 SVZ/IZ samples.* ***C)*** *Violin plot comparing dataset of proteins exclusively identified in CP (orange) with dataset of proteins exclusively identified in SVZ/IZ (blue), at E16.5. N = 1 embryos, n = 1 CP samples, 1 SVZ/IZ samples.*

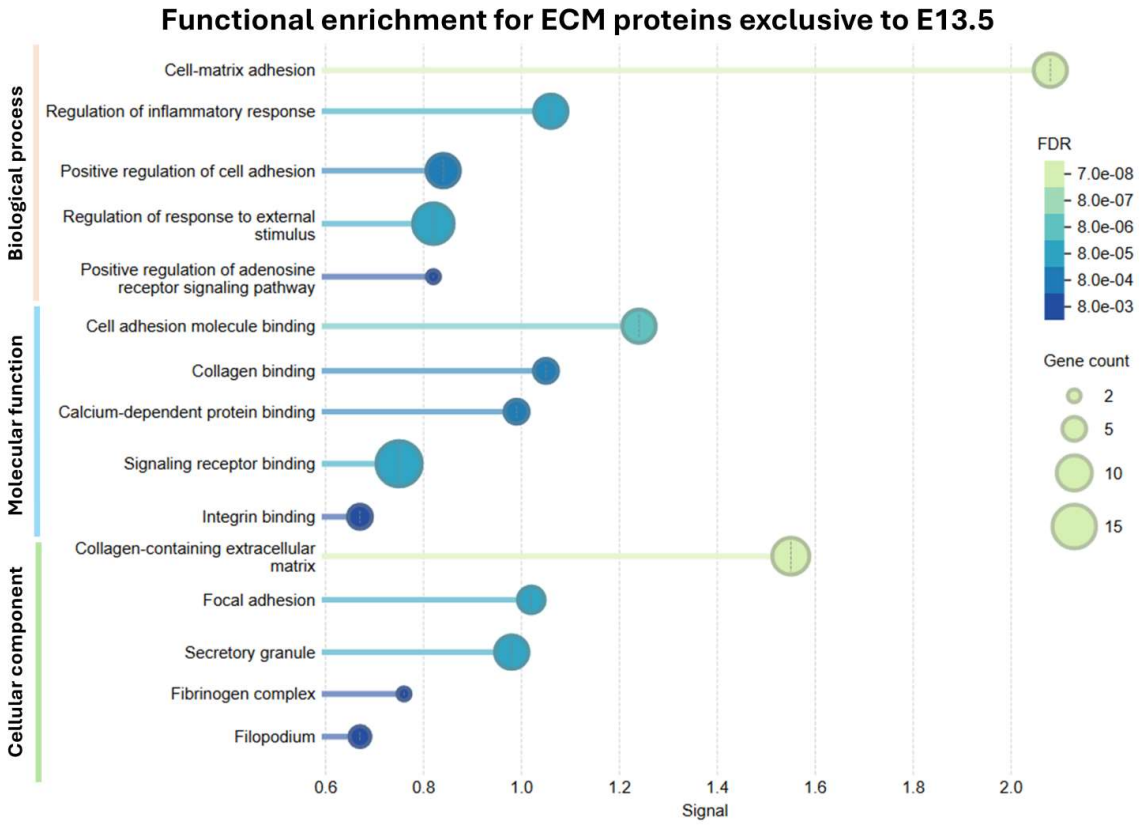

Supplementary Figure 2: ***Visualization of functional enrichment analysis of ECM-related proteins exclusively detected at E13.5.*** *N = 5 embryos, n = 5 CP samples, 5 SVZ/IZ samples per embryo.*